applied sciences

MDPI

Article

The Effect of Different Fiber Reinforcement on Bearing Capacity under Strip Foundation on the Sand Soil: An Experimental Investigation

Bilge Aksu Alcan [1,*] and Semet Çelik [2]

[1] Department of Civil Engineering, Kafkas University, 36100 Kars, Turkey
[2] Department of Civil Engineering, Atatürk University, 25240 Erzurum, Turkey; scelik@atauni.edu.tr
* Correspondence: bilge.aksu@kafkas.edu.tr

Abstract: The aim of this study is to investigate the bearing capacity-settlement behavior of strip footing settling on sand soil randomly reinforced with glass fiber, basalt fiber, macromesh fiber, and four different hybrid fiber additives in which these fibers are used together. Model tests were carried out in the laboratory on the strip footing and placed on the unreinforced and reinforced sand with different fibers. In the study, model tests were carried out on seven types of randomly reinforced soils by using glass, basalt, macrame, and mixtures of these fibers as reinforcement. In the model tests, two different fiber contents, 1% and 2%, and two different fiber lengths, 24 mm and 48 mm, were used. Tests were carried out with Dr = 30% and 50% relative density, and reinforcement depths 1B, 2B, and 3B were selected. In addition, the photographs taken during the test were analyzed with the particle image velocimetry (PIV) method and the displacements on the soil were examined. As a result of the reinforced and unreinforced model tests, the highest ultimate bearing capacity was measured as 680 kPa from the tests with Dr = 50% relative density, 48 mm length, 2% contents, and 3B depth macromesh fiber reinforced. In hybrid fibers, the highest ultimate bearing capacity was measured as 495 kPa, with Dr = 50% relative density, 48 mm length, 2% contents, and 2D depth micromesh and basalt fiber-reinforced tests. In the reinforced tests, it was concluded that the most effective fiber on bearing capacity is macromesh fiber. It can be seen that in the PIV analysis, as the fiber additive increased, the settlements made by the foundation decreased under the same pressure. It has also been observed that adding reinforcement to the soil transfers the stresses occurring in the soil to a wider area.

Keywords: basalt fiber; glass fiber; macro-synthetic fiber; hybrid fiber; bearing capacity ratio; randomly reinforced soil; PIV

check for updates

Citation: Aksu Alcan, B.; Çelik, S. The Effect of Different Fiber Reinforcement on Bearing Capacity under Strip Foundation on the Sand Soil: An Experimental Investigation. *Appl. Sci.* **2023**, *13*, 9769. https://doi.org/10.3390/app13179769

Academic Editors: Xianwei Zhang, Xinyu Liu and Ran An

Received: 1 August 2023
Revised: 25 August 2023
Accepted: 28 August 2023
Published: 29 August 2023

Copyright: © 2023 by the authors. Licensee MDPI, Basel, Switzerland. This article is an open access article distributed under the terms and conditions of the Creative Commons Attribution (CC BY) license (https://creativecommons.org/licenses/by/4.0/).

1. Introduction

The concept and principle of soil reinforcement were first developed by Vidal in 1969 when he found that adding reinforcements to a soil mass increases the shear strength of soil [1]. The reinforcing effect of fibers in soil reinforcement was first noticed by Waldron in 1977, when he observed that natural root fibers contribute to the improvement in soil strength due to their reinforcing effect [2]. In general, in fiber-reinforced soils, it has been observed that the added fiber can improve the mechanical properties of the soil due to the interface friction between the fiber and the soil. That is, the shear stresses in the soil actuate the tensile strength in the fibers and, as a result, give the soil more strength [3–5]. Randomly Distributed Fiber-reinforced Soil (RDFS) is a soil improvement technique in which fibers of desired properties and quantities are randomly ordered and compacted in place [6]. The RDFS method has become more popular in recent studies. Short staple fibers can be easily added and mixed into the soil such as cement, lime, or other additives. In this way, planes of weakness do not occur in the soil and an isotropic increase in the strength of the soil composite can be achieved [7,8].

Glass fiber improves the mechanical properties of the reinforced soil matrix such as flexural and tensile strength. They contribute to the flexibility of the soil matrix they are supplemented with and have a long period of use [9,10]. Glass fiber-reinforced sandy soil matrices have attracted great interest in many applications because of their relatively low weight, low cost, and good mechanical properties, which are desirable characteristics of natural fibers [11,12]. Philley et al. [13], in this study, first stabilized the soil with Class F fly ash and cement to improve the strength properties of the weak local soil and then reinforced it with glass fiber reinforcement. In the study, different mixtures were prepared with varying ratios such as fly ash (10, 30, 50), cement (0.5%, 1, 1.5, 2%), and glass fiber (0.25%, 0.5 and 1%). It was observed that there was a significant improvement in the pressure and shear strength parameters in the optimum additive percentage determined for all three materials. Benzian et al. [14] conducted direct shear box tests for their study to examine the effect of material properties and fiber content on the shear resistance of sand. In the study, glass fiber, polypropylene fiber, and sisal fiber were randomly reinforced into the soil mass at 50% relative density, 0.25%, 0.5, 0.75, and 1 ratio. It was observed that samples reinforced with sisal fibers had a more significant increase in strength parameters than samples reinforced with glass or polypropylene fibers. The reason one of the fiber types used in the experimental study was chosen as glass fiber is that it was thought to be suitable for comparing the results with basalt and macromesh fibers, as it is a familiar material that has been studied in the past.

Basalt fiber has high performance, natural compatibility, electrical insulation, corrosion, high temperature, and acid and alkali resistance [15,16]. When the studies in the literature are examined, it has been seen that it is widely used in thermoset resin and concrete as insulation, sound absorption, heat resistant materials, and reinforced materials [17,18]. In addition, the mechanical properties of basalt fiber such as tensile strength and modulus of elasticity, are much higher than polypropylene fiber [19,20]. Many studies have been carried out on concretes in which basalt fiber is used as an admixture. However, the use of basalt fiber additives in soil-related studies is relatively low [21]. Kale et al. [16] used three different lengths of fiber (12 mm, 18 mm, and 24 mm) to investigate the effect of basalt fiber additive on improving soil properties. They added 12 mm and 18 mm long fibers to the ground at a rate of 1.5%, 3%, 4.5%, 6%, and 24 mm long fibers at a rate of 1.5%, 2%, 2.5%, and 3% by weight. Xu et al. [22] reinforced loess soil with poor mechanical properties with basalt fiber additives in three different fiber lengths (6 mm, 12 mm, and 18 mm) and four different fiber contents (0.3%, 0.6%, 0.8%, and 1.0%). The maximum increase in strength was observed in the experimental group with a fiber content of 0.6% with a length of 12 mm, and it was determined that the shear strength of leucine of basalt fiber was improved. In their study, Mukhtar and Kumar [23] showed that the addition of basalt fiber to the local soil sample located in the Srinagar region increases the strength of the soil by decreasing the liquid limit and plastic limit, and improves the properties of the soil by decreasing the plasticity index by 62.64%. Chen et al. [24] concluded that the use of glass fiber and basalt fiber would be effective as reinforcement for higher bearing capacity and fewer cracks in granite residual soil. In their studies, fiber contents were chosen as 3%, 4%, and 5%, respectively, and fiber lengths were used as 6 mm, 9 mm, and 12 mm, respectively. While most of the studies on soil cover fine-grained soil groups, studies on cohesion-free sand soils are insufficient. Therefore, it is particularly important to study basalt fiber-reinforced cohesionless sand soil.

Macromesh fiber is a polypropylene (99%)-based macro synthetic fiber reinforcement in copolymer structure. It is variously named macro polypropylene fiber, spun polypropylene fiber, high-performance polypropylene fiber, macro synthetic fiber, and macro synthetic twisted bundle fiber [25]. They are environmentally friendly and new-generation reinforcements produced from high-performance polypropylene raw materials and have a longer life than traditional reinforcements [26,27]. In recent years, its effect on fiber-reinforced strengthening studies has begun to be investigated. Brasse et al. [28] strengthened the soil-cement composites made with cohesionless soil with the addition of single fibrillated-tapes

polypropylene fibers (SFPF) and bundles of coiled fibrillated-tapes polypropylene fibers (BCFPF) and showed that the polypropylene fiber reinforcements used had a significant effect on the bending behavior. Daneshfar et al. [29], twisted, barchip, and fibrillated, three different macro polypropylene fibers were added to the concrete in three different volume ratios 0.2%, 0.4%, and 0.6%, and the reinforcement of macro PP fibers affected the ductility behavior and ductility of the concrete. investigated the effect on mechanical properties. According to the results, the twisted, and barchip fiber-reinforced concrete has higher compressive strength than the fibrillated fiber. It has been studied mostly on concrete and polymer composites but the studies on their effects on soil are few [30,31].

A single fiber type chosen as an additive in fiber additives can often significantly improve one or more of the material's properties. However, each type of fiber often has some weak points. For example, filament fiber can improve tensile strength but has the problem of poor dispersion. Therefore, recently researchers have mixed different fiber types to take full advantage of the reinforcing effect of each fiber especially in the field of concrete. Studies have been carried out in different combinations such as polymer-polymer hybrid fiber and polymer-natural hybrid fiber, steel-steel hybrid fiber, and steel-polymer hybrid fiber [32,33]. As a result of the studies, it has been seen that hybrid fibers can improve the toughness, ductility, energy dissipation capacity, and durability performance of concrete [30,34]. When the existing studies on improvement with fiber additives are evaluated, the effects on the soil are examined as a result of the addition of one or more fibers to the soil separately under various varying conditions [35–37]. However, studies on the effect of using two or more fibers together in a hybrid form on soil are very insufficient.

This study is aimed to contribute to the deficiencies in the literature mentioned above. In this context, an average of 300 laboratory model tests were carried out to investigate the effect of glass fiber, basalt fiber, macromesh fiber, and hybrid fiber-reinforced soils where these three fibers are used together in different combinations on the bearing capacity. In the experimental study, the scope of the study was expanded by investigating the effect of fiber length, fiber content, depth of reinforcement layer, and different relative density values, as well as fiber type. To investigate the effect of fiber length, two different fiber lengths of 24 mm and 48 mm were used. To see the effect of fiber content, fiber additives with two different contents of 1% and 2% were investigated. To see the effect of relative density, tests were carried out on soils with 30% and 50% relative density. In addition, soils were reinforced with fiber at depths of (B) 1, 2, and 3 times the foundation width, and the effect of three different reinforcement depths on soil stabilization was evaluated. Finally, to analyze the sand soil settlement behavior strengthened with different fiber types under varying environmental conditions within the scope of the study, the GeoPIV-RG program, an image analysis module running on MATLAB was used. For the image analysis of each test, a series of photographs taken at regular intervals during the test were used as data.

2. Materials and Methods

2.1. Test Materials

2.1.1. Soil Samples

Sieve analysis was performed in accordance with ASTM D2487 [38] standards to determine the grain diameter distribution of the soil used in experimental studies. The grain diameter distribution curve of the sand soil used in the experimental study is given in Figure 1. According to the Unified Soil Classification System (USCS), the soil class is determined as poorly graded (uniform) sand (SP). The granulometry parameters of the sand used in the tests are given in Table 1.

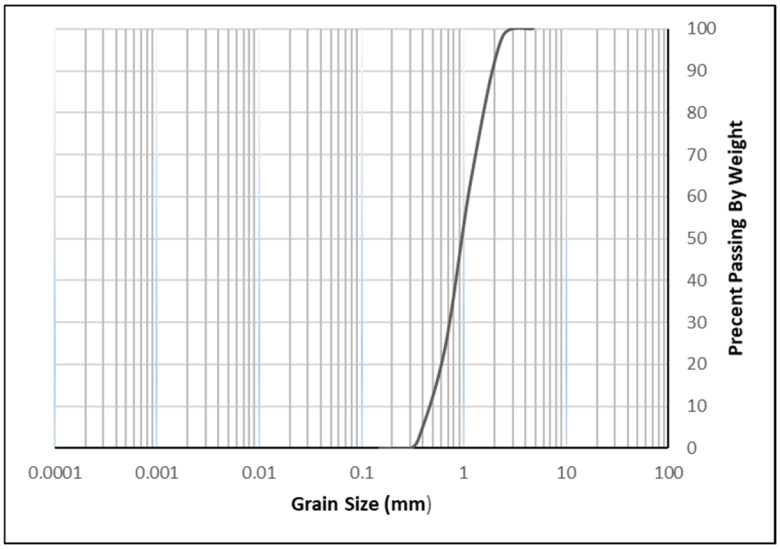


Figure 1. Grain size distribution of sand soil.

Table 1. Sieve analysis results of sand soil used in experimental study.

Granulometry Parameters	Value
D_{10}, Effective grain size (mm)	0.47
D_{30} (mm)	0.7
D_{60} (mm)	1.1
C_u (D_{60}/D_{10}), Coefficient of uniformity	2.34
C_c ($D_{30}^2/(D_{60}\cdot D_{10})$), Coefficient of curvature	0.95

In this study, model loading tests at approximately 30% and 50% relative density were performed. The index properties of sand for 30% and 50% relative densities are given in Table 2. Shear box (direct shear) tests were carried out in accordance with ASTM D 3080 [39] standard. The sand soil was placed in a Shear box cell with dimensions of 60 mm × 60 mm and a height of 38 mm at relative densities to be used in tests. Then, the soil sample was sheared horizontally by pushing on the bottom ring while holding the top ring under normal stresses of 30 kPa, 60 kPa, and 120 kPa, respectively. The sharing speed is set to 1 mm/min. According to the shear test results, the shear strength angle was obtained as $\phi = 32.1^\circ$ for Dr = 30% relative density and as $\phi = 40.1^\circ$ for Dr = 50% relative density.

Table 2. Index properties of poorly graded sand soil used in model tests.

Relative Density Parameters	Value
Specific gravity (G_s)	2.71
Maximum void ratio (e_{max})	0.84
Maximum dry unit weight (γ_{kmax}) (kN/m^3)	17.93
Minimum void ratio (e_{min})	0.47
Minimum dry unit weight (γ_{kmin}) (kN/m^3)	14.40
Void ratio (e) (Dr = 30%)	0.73
Void ratio (e) (Dr = 50%)	0.65
Dry unit weight (γ_k) (kN/m^3) (Dr = 30%)	15.30
Dry unit weight (γ_k) (kN/m^3) (Dr = 50%)	15.96

2.1.2. Fibers

Basalt fibers, glass fiber, and macromesh fibers used in the tests are shown in Figure 2. The physical and mechanical properties of the fibers used in the study are given in Table 3.

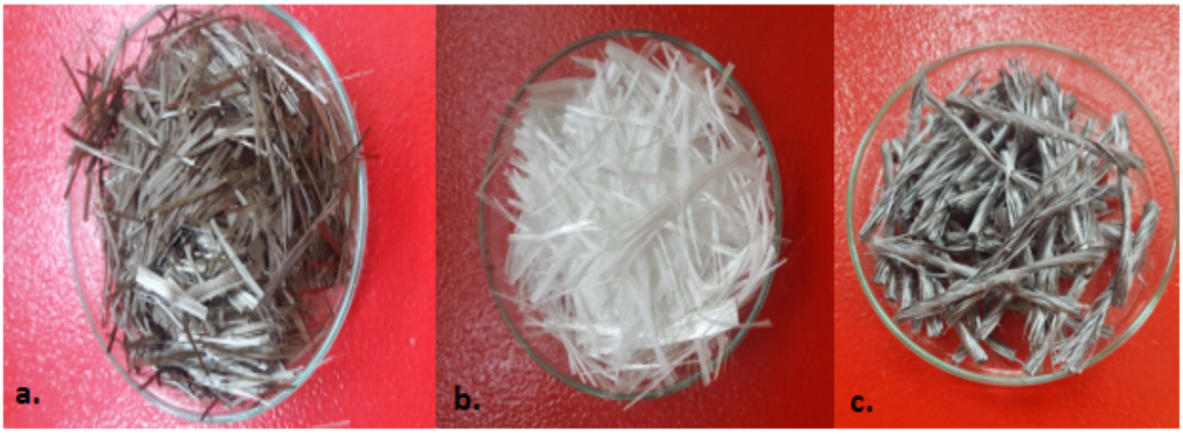


Figure 2. Material diagram; (**a**) Basalt fiber; (**b**) Glass fiber; (**c**) Macromesh fiber.

Table 3. Physical and mechanical properties of basalt fiber, glass fiber, and macromesh fiber.

Properties	Basalt Fiber	Glass Fiber	Macromesh Fiber
Fiber type	Micro	Micro	Macro
Length (mm)	24	24/48	24/48
Average diameter (μm)	16	14	850
Specific gravity (G)	2.65	2.60	0.91
Young's modulus (GPa)	89	77	5.75
Breaking tensile strength (MPa)	4840	3400	750

2.2. Experimental Setup

The model tank has a length of 1000 mm, a width of 300 mm, and a height of 1000 mm. The front is made of 20 mm thick glass fiber to display the displacement of the soil during loading, and the back and sides are made of sheet steel. Experimental studies were carried out under plane strain conditions using a strip foundation. For the model foundation, a rigid steel plate with a length of L = 300 mm, a height of H = 20 mm, and a width of B = 100 mm was used. The surfaces of the foundation in contact with the tank are covered with thick rubber material to reduce the friction coefficient. Based on the model, a hydraulic jack that can load up to 5000 kg according to the desired speed is used. To check the centric loading, two Linear Variable Differential Transformers (LVDT) were placed diagonally at the two corners of the footing plate and settlements were read. In the tests, an S-type load cell with a capacity of 5000 kg was used to determine the load values on the model base plate. During the tests, the settlements and stress values from the load cells and LVDTs were transferred to the data collection device and converted into numerical values. The schematic of the experimental setup is given in Figure 3.

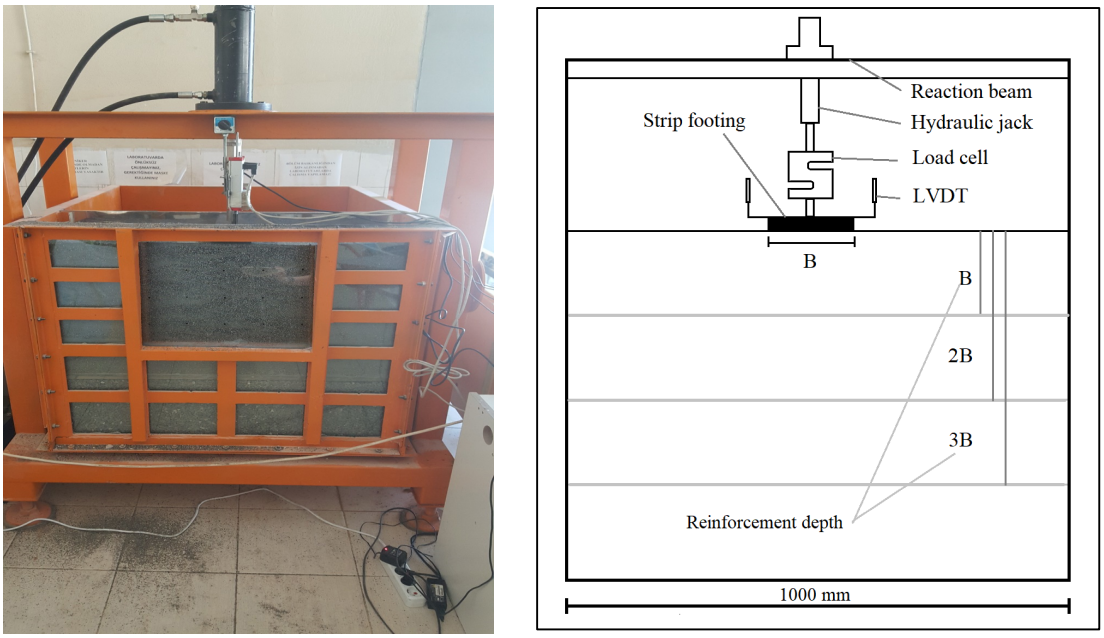


Figure 3. (**a**) Photograph of the model tank, and (**b**) schematic shape of the model tank.

2.3. Test Program

Relative density has a great influence on the mechanical behavior of sands. Soils with low relative density are more likely to have settlement and bearing capacity problems. For this reason, loose (Dr = 30%) and medium-dense (Dr = 50%) soils were preferred to stabilize them with fiber additives. In the experimental study, firstly, loading tests were performed on model strip footing at 30% and 50% relative density in unreinforced soil, and ultimate bearing capacity was determined. Then, an experimental program was prepared for the reinforced soil tests. While determining the ultimate bearing capacity, there are options such as the 0.1B method (B is the width of model footing) [40], the tangential intercept method [41], the log-log method [42], and the hyperbolic method, apart from using load-deformation curves [43]. In the experimental studies, especially on reinforced soils, the 0.1B method was used. While determining the experimental study program, six parameters were taken into account. While determining the experimental study program, six parameters were taken into account. These parameters are two different relative densities (Dr = 30% and Dr = 50%), two different fiber contents (Fc = 1% and Fc = 2%), three different fiber additives (glass fiber, basalt fiber, and macromesh fiber), four different hybrid fiber additives (glass + basalt, basalt + macromesh, glass + macromesh, and glass + basalt + macromesh), two different fiber lengths (Fl = 24 mm and Fl = 48 mm), and three different reinforcement depths (B, 2B, and 3B). In the experimental study, 120 experimental groups were formed with the parameters given above. The representation of these groups is given in Table 4. When using hybrid fibers, fibers in each group were mixed in equal percentages. The randomly distributed fiber-reinforced sand soil with a relative density of 30% and 50% were placed in the tank in horizontal layers of 5 cm. To provide the desired relative density, the glass surface of the test tank was scaled from the outside, and the required sand and fiber weight for each layer was calculated in advance, mixed manually (by hand), and placed in the tank in a controlled manner.

Table 4. Test program.

		Fl = 24 mm		**Fl = 48 mm**		
Dr = 30%	Fc = 1%	7 group	B	3 group	B	(24 mm 7 group;
			2B		2B	1-glass
			3B		3B	2-macromesh
	Fc = 2%	7 group	B	3 group	B	3-basalt
			2B		2B	4-glass + macromesh
			3B		3B	5-glass + basalt
Dr = 50%	Fc = 1%	7 group	B	3 group	B	6-macromesh + basalt
			2B		2B	7-glass + macromesh + basalt
			3B		3B	48 mm 3 group;
	Fc = 2%	7 group	B	3 group	B	1-glass
			2B		2B	2-macromesh
			3B		3B	3-glass + macromesh)
Total		84 group		36 group		120 group

2.4. GeoPIV Analysis

GeoPIV-RG application was used for the analysis of the images obtained from the experimental studies. GeoPIV-RG is designed for geotechnical research applications and is used in the analysis of problems involving large displacements and deformations. It is capable of sub-pixel measurement resolution. At least a 10-fold improvement in measurement accuracy was achieved over the most widely used particle image velocimetry (PIV) approach for all deformation modes including rigid body displacements, rotations, and strains (compression and share) [44].

In our study, GeoPIV-RG software was used to analyze the settlement formed as a result of loading under model strip footing for each of the unreinforced and reinforced soil groups. GeoPIV-RG: It is an image analysis module designed for geotechnical research applications, running under the MATLAB R2019B program. To perform the analysis, a fixed camera was placed in front of the test tank and pictures were taken at regular intervals from the moment the soil was loaded. The basic principle of PIV is to look for changes in the analysis points of images taken at different times. The cross-correlation function can be calculated using the Fast Fourier Transform (FFT) to match the analysis points and obtain the motion states. The normalized cross-correlation function can be expressed as

$$R(m,n) = \frac{\sum_i \sum_j u(i,j) \cdot v(i+m, j+n)}{\sqrt{\sum_i \sum_j u^2(i,j) \sum_i \sum_j v^2(i+m, j+n)}} \quad (1)$$

Here, m, given in Equation 1 represents displacements in the horizontal direction, n represents the displacements in the vertical direction, $u(I,j)$ and $v(I,j)$ represent the gray distribution functions of the image before and after deformation [45]. The pictures taken during the tests were analyzed with the GeoPIV-RG software and the displacements in the soil were obtained. In the program, certain points are selected in the first picture. The program has divided the first image entered as data into very small areas. FFT was then used to compare each area with subsequent images in sequence. As a result of the subsequent analyses, the program obtained image processing results such as vector displacement, horizontal displacement, vertical displacement, general displacement, and stress distributions of the soil from the movement of soil particles (Figure 4).

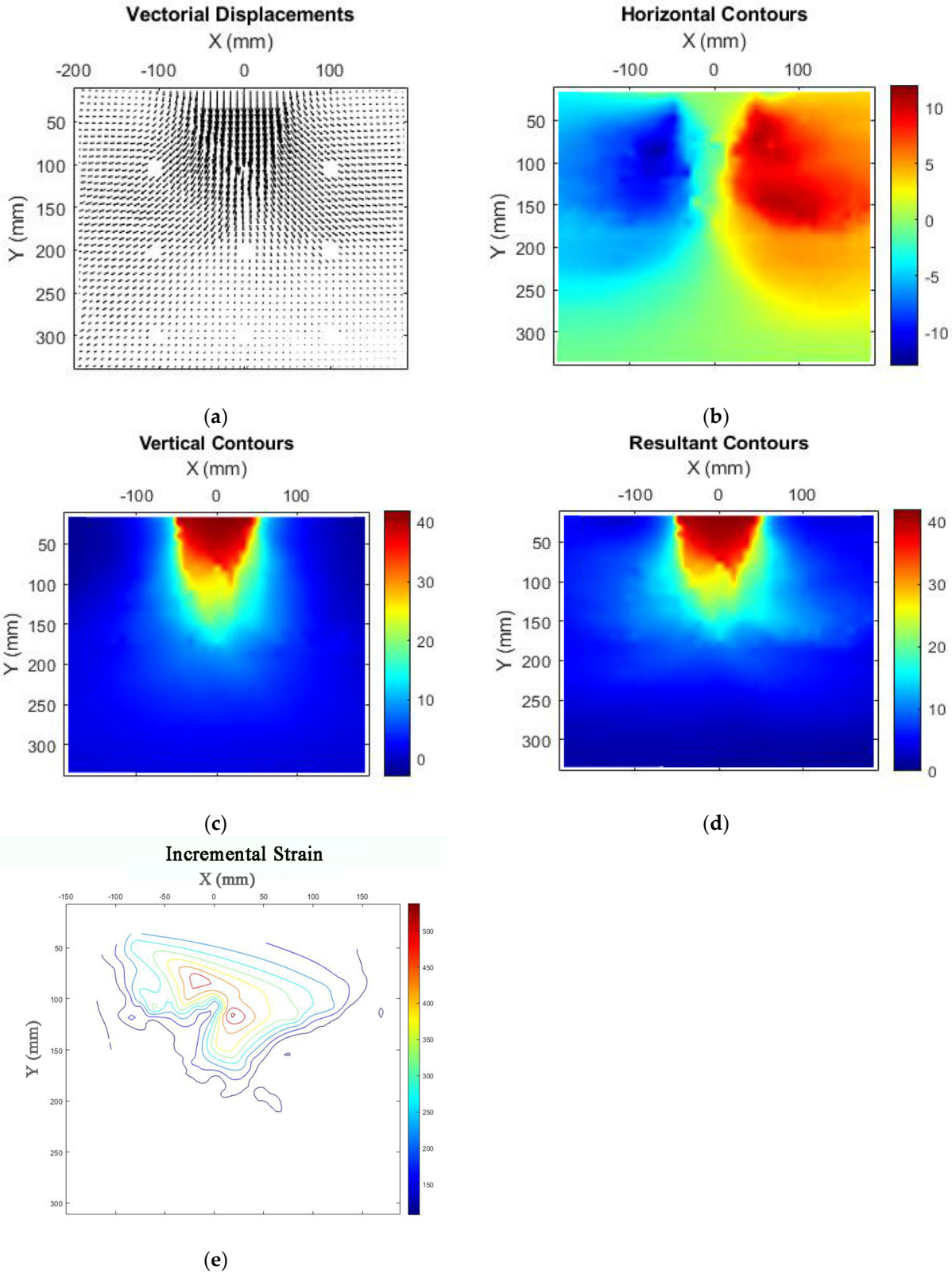


Figure 4. PIV results: (**a**) Vectorial displacements; (**b**) horizontal contours; (**c**) vertical contours; (**d**) resultant contours; (**e**) incremental strain.

3. Results Analysis and Discussion

The base pressure settlement curves obtained in this study as a result of the evaluation of other parameters according to fiber types and the corresponding bearing capacity ratio values were obtained as follows.

Glass Fiber;

The average base pressure-settlement curves obtained according to different fiber lengths, different fiber percentages, and different reinforcement layer depths as a result of model loading tests on sand soil randomly reinforced with glass fiber at Dr = 30% and Dr = 50% are shown in Figure 5, and the reinforcement depth-bearing capacity ratio relationship is given in Figure 6.

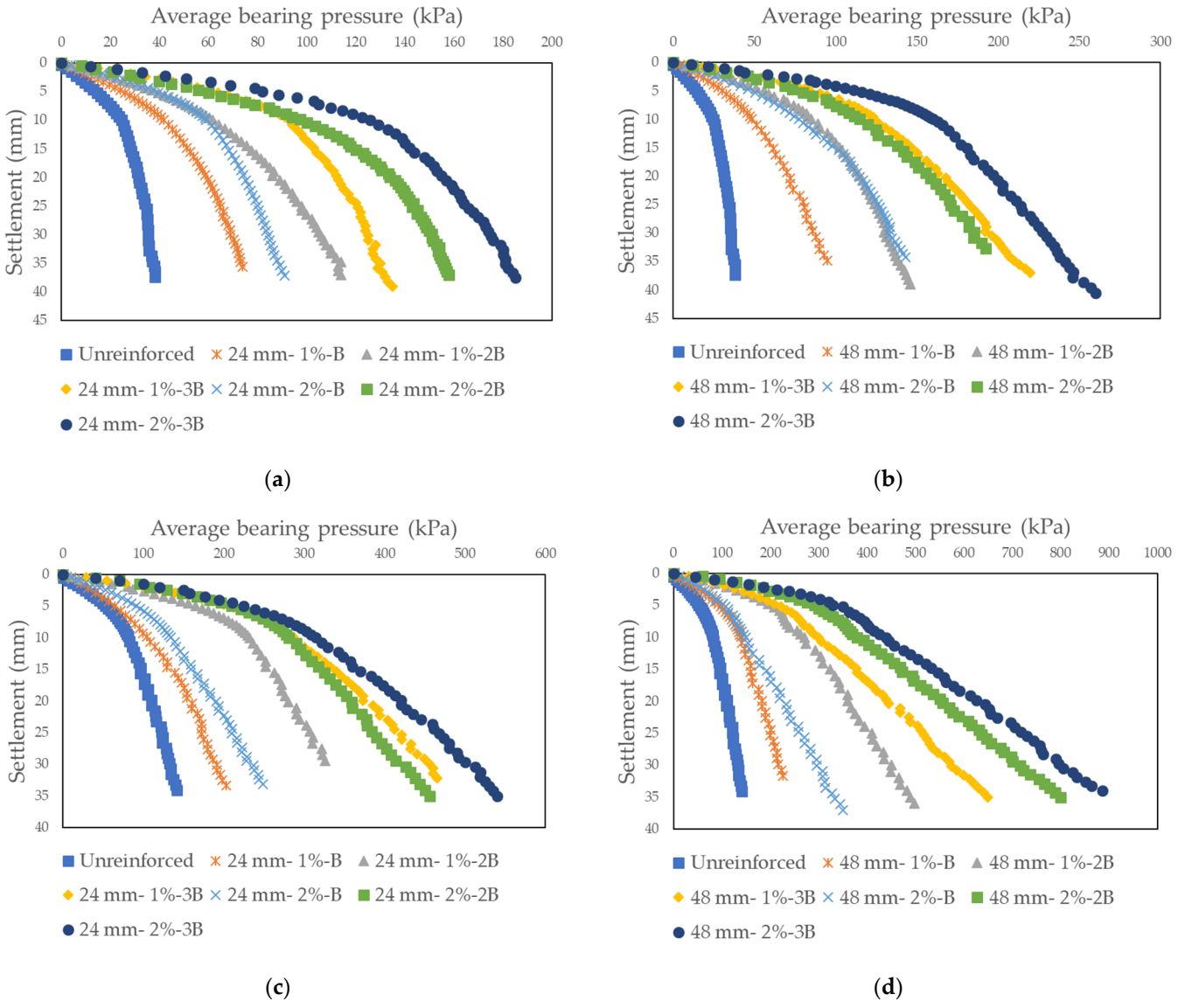


Figure 5. Average base pressure-settlement curves obtained as a result of model tests on sand soil randomly reinforced with glass fiber: (**a**) Dr = 30%, Fl = 24 mm; (**b**) Dr = 30%, Fl = 48 mm; (**c**) Dr = 50%, Fl = 24 mm; (**d**) Dr = 50%, Fl = 48 mm.

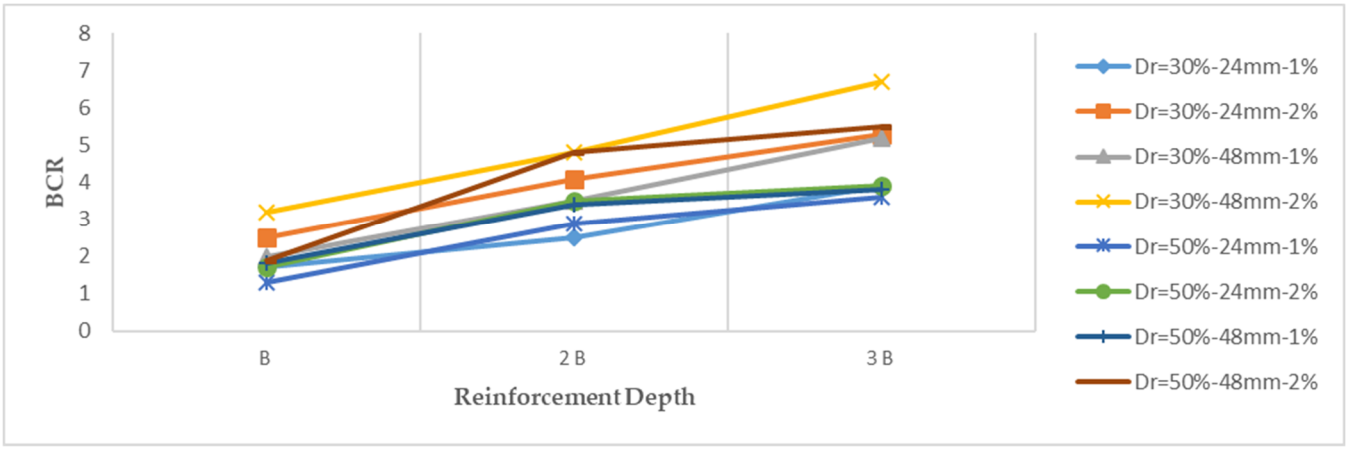


Figure 6. Variation of bearing capacity ratio (BCR) with reinforcement depth (Dr = 30–50%, Fl = 24–48 mm, Fc = 1–2%, and glass fiber).

- In glass fiber-reinforced soils, the highest ultimate bearing capacity (qu) was determined as 440 kPa in the case of adding glass fiber to the sand at Dr = 50%, Fc = 2%, Fl = 48 mm, and 3B reinforcement depth. The highest bearing capacity ratio (BCR = final bearing capacity of reinforced soil/final bearing capacity of unreinforced soil) was determined as 6.7 by adding glass fiber to sand at Dr = 30%, Fc = 2%, Fl = 48 mm, 3B reinforcement depth.
- For all fiber lengths and percentages at Dr = 30%, there was a 48–73% increase in BCR when reinforcement depth was changed from B to 2B, and there was a 30–52% increase in BCR when changed from 2B to 3B. At Dr = 50%, there was a 94–153% increase in BCR for all reinforcement lengths and percentages from depth B to 2B and an 11–23% increase in BCR from 2B to 3B. Changing the reinforcement depth from 2B to 3B at Dr = 50% had no effect on ultimate bearing capacity as much as the percentage increase seen at Dr = 30%.
- Changing the glass fiber length from 24 mm to 48 mm at all reinforcement depths and contents at Dr = 30% increased the BCR in the range of 16–39%. Changing the content of reinforcement from 1% to 2% at all reinforcement depths and lengths increased the BCR between 28% and 61%. Changing the glass fiber length from 24 mm to 48 mm at all reinforcement depths and percentages at Dr = 50% increased BCR in the range of 5–41%. Changing the percentage of reinforcement from 1% to 2% at all reinforcement depths and lengths increased the BCR between 6% and 45%. The increase in bearing capacity ratios obtained as a result of increasing the fiber length from 24 mm to 48 mm by increasing the fiber percentage from 1% to 2% in 50% relative density glass fiber-reinforced soils is similar. However, the increase in BCR obtained as a result of increasing fiber content in soils with 30% relative density glass fiber is higher than the increase in BCR obtained as a result of increasing fiber length.

Macromesh Fiber

The average base pressure-settlement curves obtained according to different fiber lengths, different fiber percentages, and different reinforcement layer depths as a result of model loading tests on sand soil randomly reinforced with macromesh fiber at Dr = 30% and Dr = 50% are shown in Figure 7, and the reinforcement depth-bearing capacity ratio relationship is given in Figure 8.

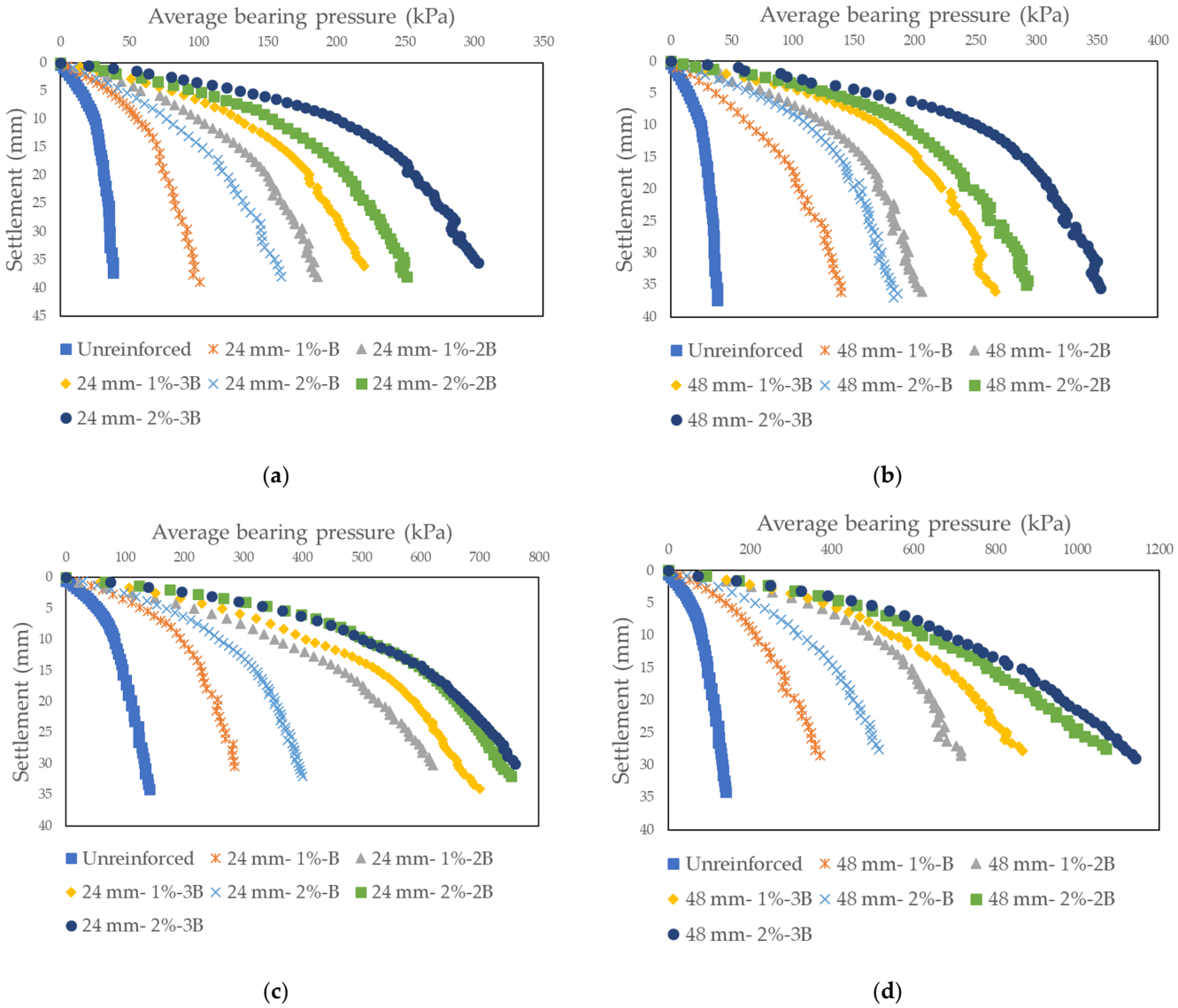


Figure 7. Average base pressure-settlement curves obtained as a result of model tests on sand soil randomly reinforced with macromesh fiber: (**a**) Dr = 30%, Fl = 24 mm; (**b**) Dr = 30%, Fl = 48 mm; (**c**) Dr = 50%, Fl = 24 mm; (**d**) Dr = 50%, Fl = 48 mm.

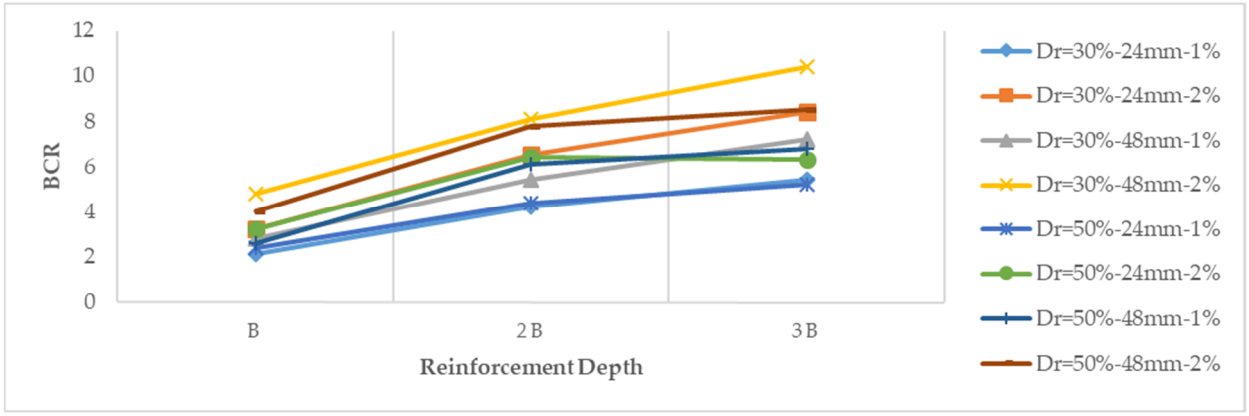


Figure 8. Variation of bearing capacity ratio (BCR) with reinforcement depth (Dr = 30–50%, Fl = 24–48 mm, Fc = 1–2%, and macromesh fiber).

- In macromesh fiber-reinforced soils, the highest ultimate bearing capacity (q_u) was determined as 680 kPa in the case of adding macromesh fiber to the sand at Dr = 50%, Fc = 2%, Fl = 48 mm, and 3B reinforcement depth. The highest BCR was determined as 10.4 by adding macromesh fiber to sand at Dr = 30%, Fc = 2%, Fl = 48 mm, 3B reinforcement depth.
- When the reinforcement depth was changed from B to 2B and from 2B to 3B for all fiber lengths and percentages at Dr = 30%, the BCR increased by 69–101% and 28–33%, respectively. For all reinforcement lengths and percentages, the BCR increased at Dr = 50% by 53–135% from depth B to 2B and by −1.5–18% from 2B to 3B. The ultimate bearing capacity did not rise by the same proportion when the reinforcement depth was increased from 2B to 3B at Dr = 50%. Especially in the experimental group with Dr = 50%, Fl = 48 mm, Fc = 2% macromesh fiber additives, when the depth was increased from 2B to 3B, there was no increase in the bearing capacity.

In both relative densities, an increase in bearing capacity was observed with increasing fiber length. The soil group, which is reinforced at depth B with Fc = 2% and examined at 30% relative density, has had the highest increase. In both relative densities, an increase in bearing capacity was observed with increasing fiber percentage.

Basalt Fiber

The average base pressure-settlement curves obtained according to different fiber percentages and different reinforcement layer depths as a result of model loading tests on sand soil randomly reinforced with basalt fiber at Dr = 30% and Dr = 50% are shown in Figure 9 and the reinforcement depth-bearing capacity ratio relationship is given in Figure 10.

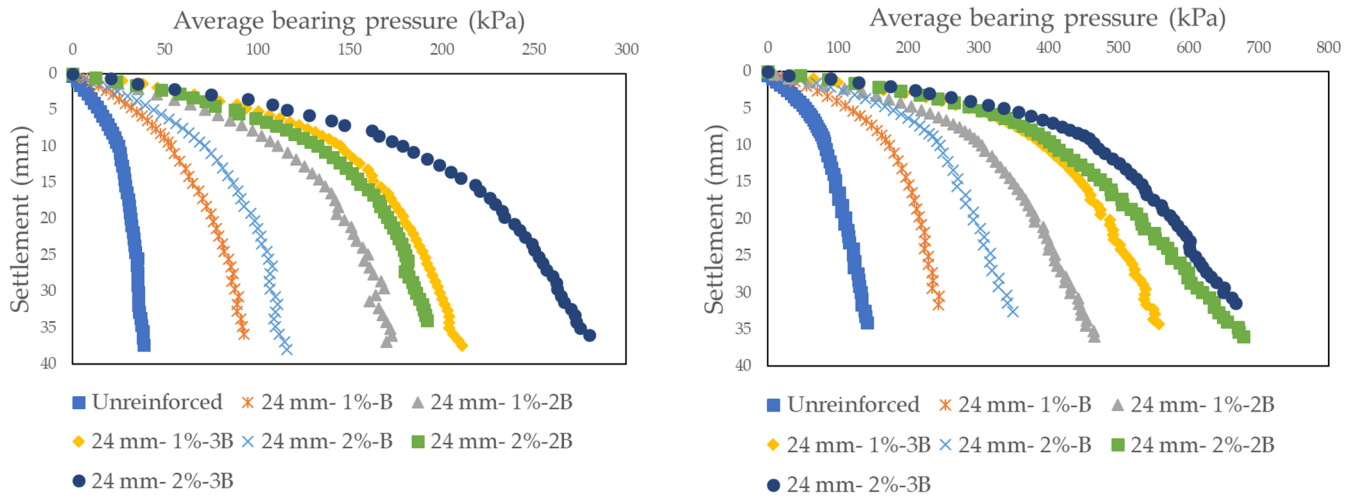


Figure 9. Average base pressure-settlement curves obtained as a result of model tests on sand soil randomly reinforced with basalt fiber: (**a**) Dr = 30%, Fl = 24 mm; (**b**) Dr = 50%, Fl = 24 mm.

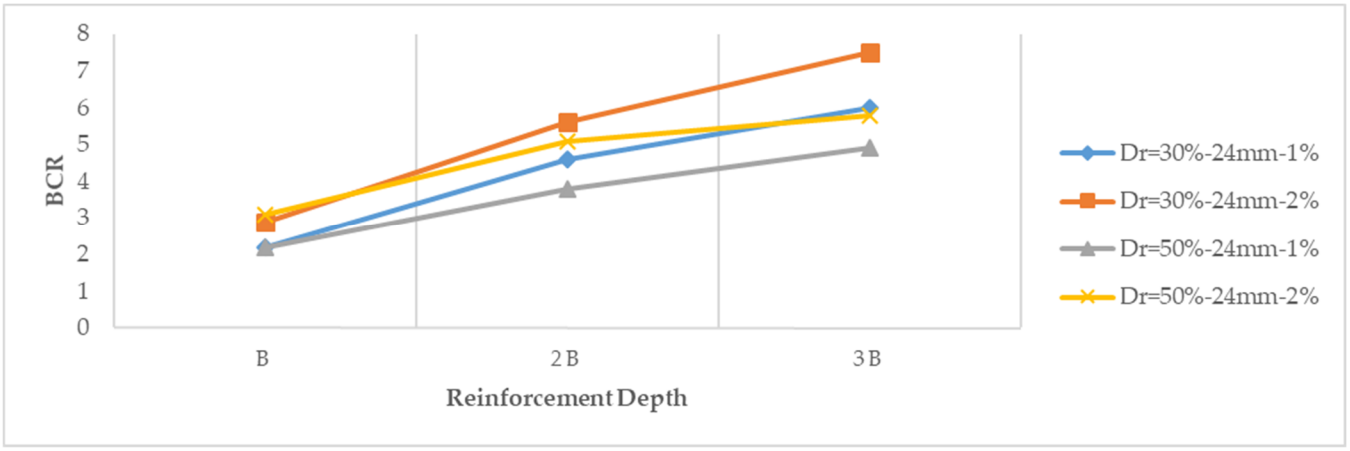
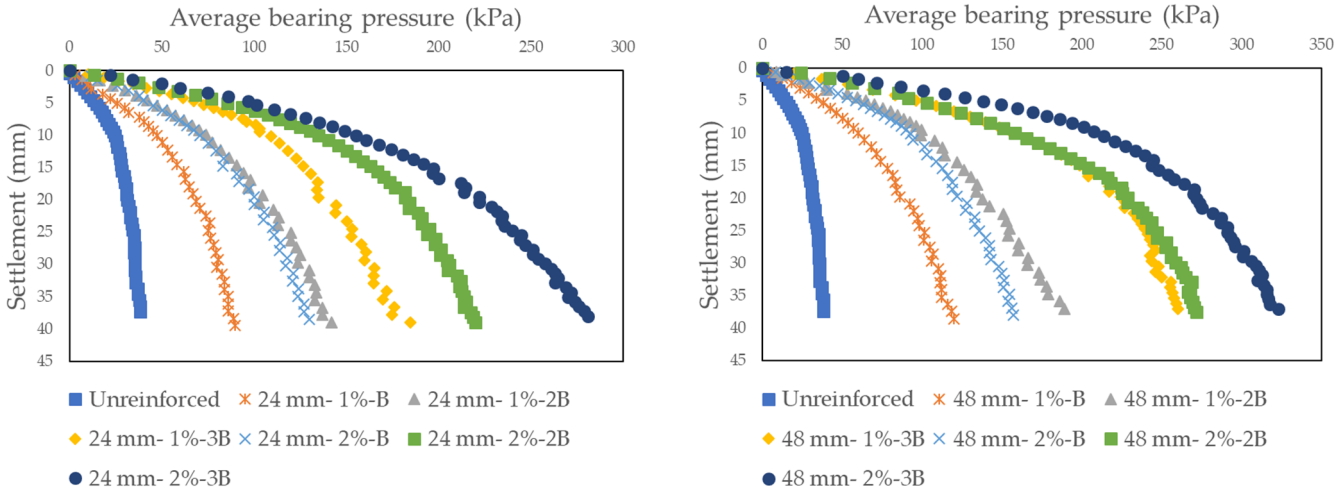


Figure 10. Variation of bearing capacity ratio (BCR) with reinforcement depth (Dr = 30–50%, Fl = 24 mm, Fc = 1–2%, and basalt fiber).

- In basalt fiber-reinforced soils, the highest ultimate bearing capacity (q_u) was determined as 467 kPa in the case of adding basalt fiber to the sand at Dr = 50%, Fc = 2%, Fl = 24 mm, and 3B reinforcement depth. The highest BCR was determined as 7.5 by adding basalt fiber to sand at Dr = 30%, Fc = 2%, Fl = 24 mm, 3B reinforcement depth.
- At both relative densities, the increase in bearing capacity is greater when reinforcement depth is increased from B to 2B. However, the impact on the ultimate bearing capacity of increasing the reinforcement depth from 2B to 3B at Dr = 50% is less significant than the percentage increase seen at Dr = 30%.

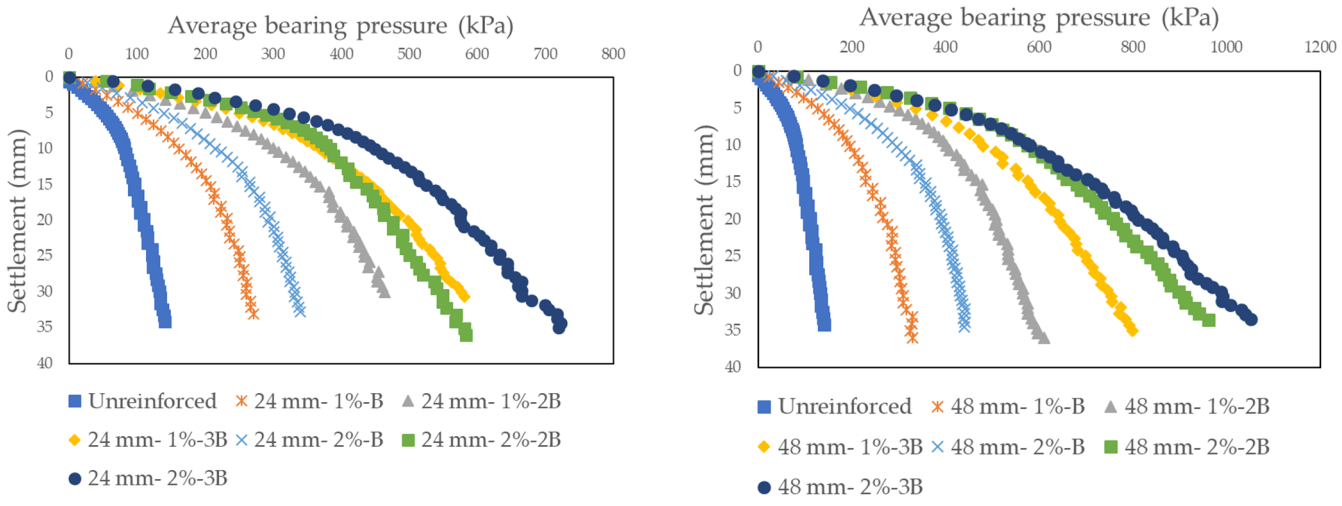
Glass + Macromesh Fiber

The average base pressure-settlement curves obtained according to different fiber lengths, different fiber contents, and different reinforcement layer depths as a result of model loading tests on sand soil randomly reinforced with glass + macromesh fiber at Dr = 30% and Dr = 50% are shown in Figure 11, and the reinforcement depth-bearing capacity ratio relationship is given in Figure 12.



(**a**) (**b**)

Figure 11. *Cont.*



(**c**) (**d**)

Figure 11. Average base pressure-settlement curves obtained as a result of model tests on sand soil randomly reinforced with glass + macromesh fiber: (**a**) Dr = 30%, Fl = 24 mm; (**b**) Dr = 30%, Fl = 48 mm; (**c**) Dr = 50%, Fl = 24 mm; (**d**) Dr = 50%, Fl = 48 mm.

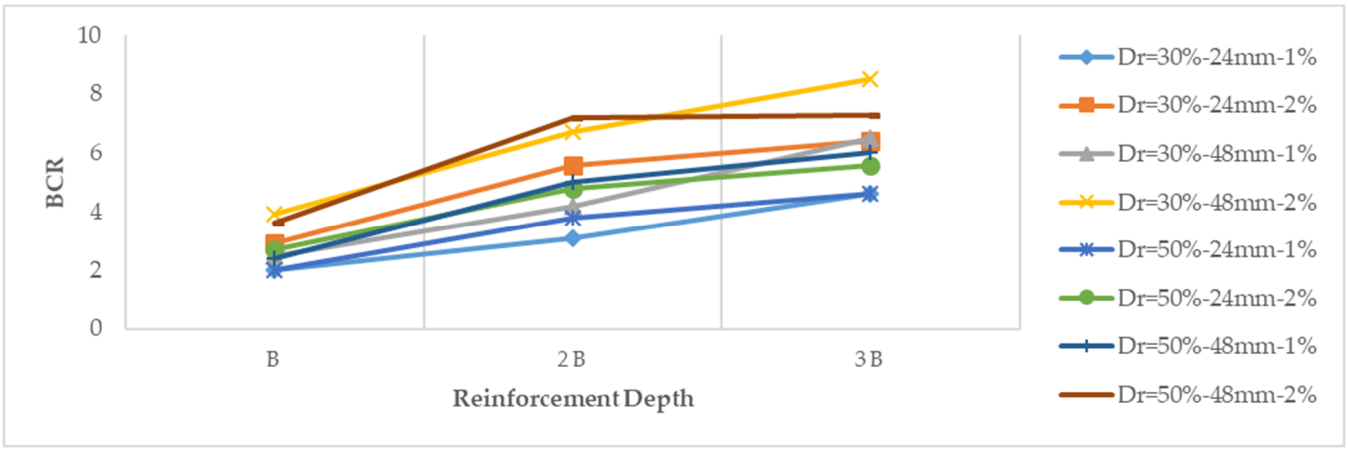


Figure 12. Variation of bearing capacity ratio (BCR) with reinforcement depth (Dr = 30–50%, Fl = 24–48 mm, Fc = 1–2%, glass and macromesh fiber).

- In glass and macromesh fiber reinforced soils, the highest ultimate bearing capacity (q_u) was determined as 580 kPa in the case of adding glass + macromesh fiber to the sand at Dr = 50%, Fc = 2%, Fl = 48 mm, and 3B reinforcement depth. The highest BCR was determined as 8.5 by adding glass + macromesh fiber to sand at Dr = 30%, Fc = 2%, Fl = 48 mm, 3B reinforcement depth.
- At 30% relative density, constant fiber content, and constant reinforcement depth, when the fiber length increases from 24 mm to 48 mm, the group with the highest increase in bearing capacity ratio is the group reinforced with glass + macromesh fiber in 3B reinforcement depth with 1% fiber content, and the rate of bearing capacity increased by 41%.
- When the soil layer depth reinforced at 30% relative density passes from 2B depth to 3B depth, the least increase in bearing capacity was observed in the 24 mm long 2% fiber-reinforced test. In both relative densities, the highest bearing strength was observed in the 48 mm long soil sample with 2% fiber reinforcement. There is almost no difference between the increase in bearing capacity as a result of improvement

in 2B depth and 3B depth in 2% fiber-reinforced soil with a length of 48 mm at 50% relative density.

Glass + Basalt Fiber

The average base pressure-settlement curves obtained according to different fiber percentages and different reinforcement layer depths as a result of model loading tests on sand soil randomly reinforced with glass + basalt fiber at Dr = 30% and Dr = 50% are shown in Figure 13 and the reinforcement depth-bearing capacity ratio relationship is given in Figure 14.

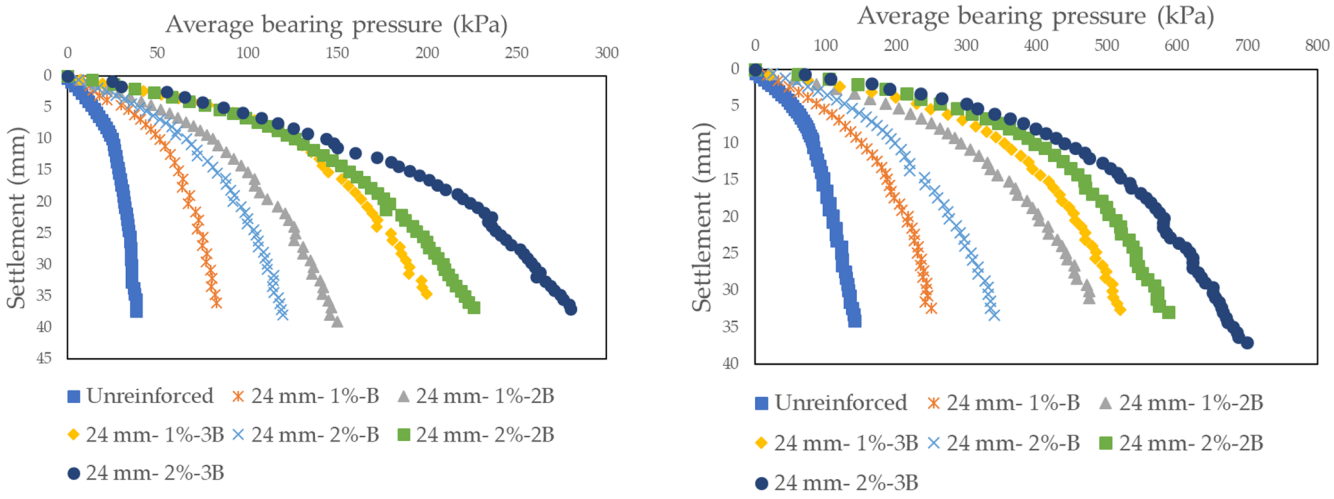


Figure 13. Average base pressure-settlement curves obtained as a result of model tests on sand soil randomly reinforced with glass + basalt fiber: (**a**) Dr = 30%, Fl = 24 mm; (**b**) Dr = 50%, Fl = 24 mm.

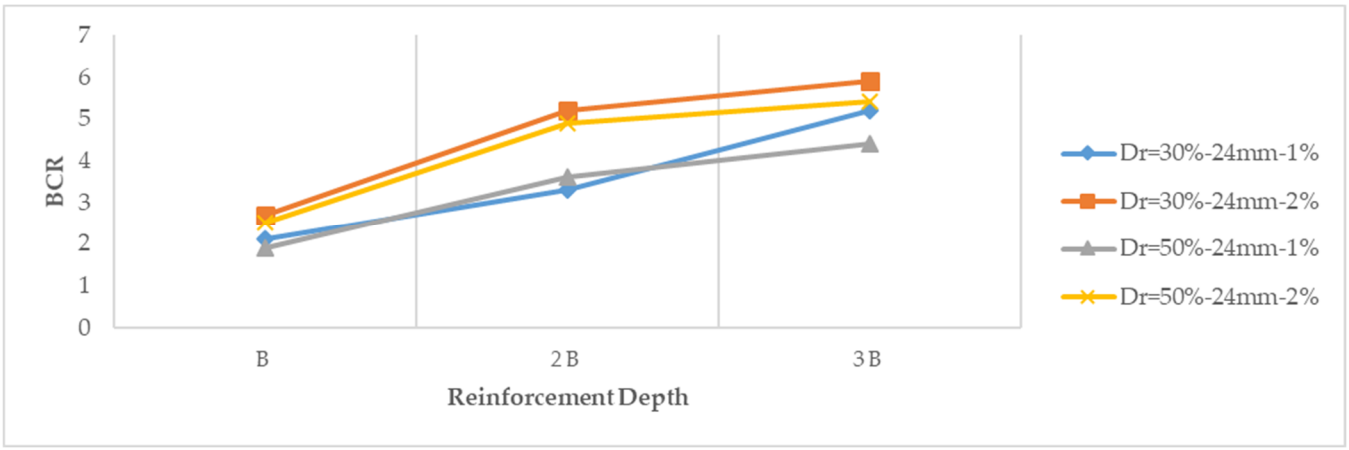


Figure 14. Variation of bearing capacity ratio (BCR) with reinforcement depth (Dr = 30–50%, Fl = 24 mm, Fc = 1–2%, glass and basalt fiber).

- In glass and basalt fiber-reinforced soils, the highest ultimate bearing capacity (q_u) was determined as 431 kPa in the case of adding glass + basalt fiber to the sand at Dr = 50%, Fc = 2%, Fl = 24 mm, and 3B reinforcement depth. The highest BCR was determined as 5.9 by adding glass + basalt fiber to sand at Dr = 30%, Fc = 2%, Fl = 24 mm, 3B reinforcement depth.
- The ultimate bearing capacity is significantly affected by increasing the reinforcement depth from B to 2B at Dr = 50%, However, the ultimate bearing capacity is little affected

by increasing the reinforcement depth from 2B to 3B. Reinforcement depth for soil reinforced with glass + basalt fiber at 50% relative density can be taken as 2B.

Macromesh + Basalt Fiber

The average base pressure-settlement curves obtained according to different fiber percentages and different reinforcement layer depths as a result of model loading tests on sand soil randomly reinforced with macromesh + basalt fiber at Dr = 30% and Dr = 50% are shown in Figure 15 and the reinforcement depth-bearing capacity ratio relationship is given in Figure 16.

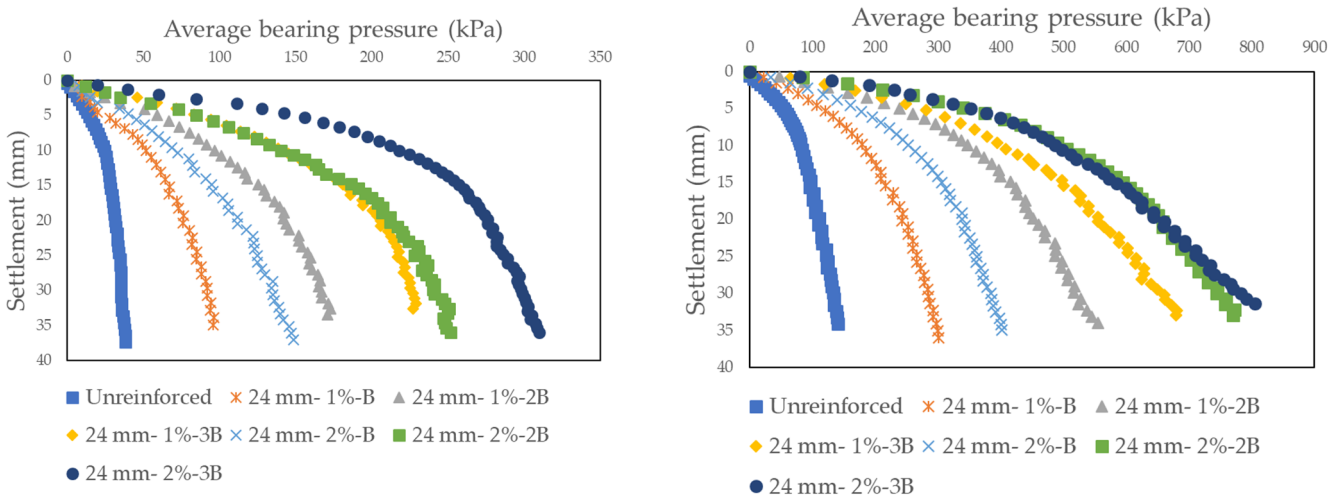


Figure 15. Average base pressure-settlement curves obtained as a result of model tests on sand soil randomly reinforced with macromesh + basalt fiber: (**a**) Dr = 30%, Fl = 24 mm; (**b**) Dr = 50%, Fl = 24 mm.

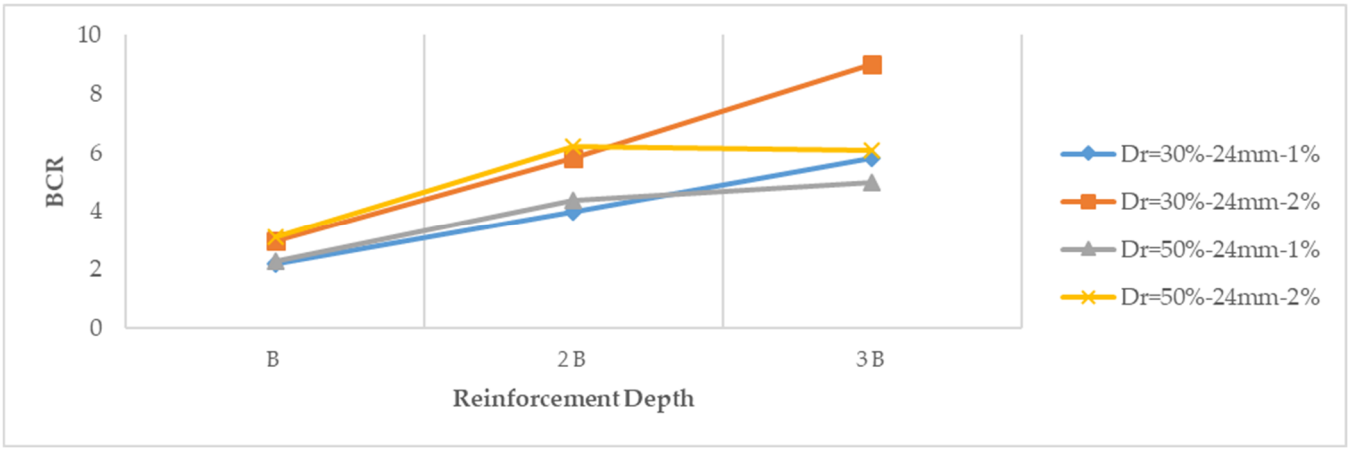


Figure 16. Variation of bearing capacity ratio (BCR) with reinforcement depth (Dr = 30–50%, Fl = 24 mm, Fc = 1–2%, macromesh and basalt fiber).

- In macromesh and basalt fiber-reinforced soils, the highest ultimate bearing capacity (q_u) was determined as 495 kPa in the case of adding macromesh + basalt fiber to the sand at Dr = 50%, Fc = 2%, Fl = 24 mm, and 3B reinforcement depth. The highest BCR was determined as 9 by adding macromesh + basalt fiber to sand at Dr = 30%, Fc = 2%, Fl = 24 mm, 3B reinforcement depth.
- For Dr = 50% Fc = 1% and 2%, basalt + macromesh fiber added experimental group showed an increase of 91% and 100% in BCR when the reinforcement depth was

increased from B to 2B, respectively, but when the reinforcement depth was increased from 2B to 3B, the increase in BCR was 14% and −1.6%, respectively. As can be seen here, when the reinforcement depth is increased from 2B to 3B in the 1% fiber added sample, the increase in the bearing capacity ratio was very low, while there was no increase in the bearing capacity ratio when the reinforcement depth was increased from 2B to 3B in the 2% fiber added sample. In fact, there was a very small decrease. Based on this, it was deemed more appropriate to choose 2B improving depth in experimental groups with 2% basalt + macromesh fiber at 50% relative density.

Glass + Macromesh + Basalt Fiber

The average base pressure-settlement curves obtained according to different fiber contents and different reinforcement layer depths as a result of model loading experiments on sand soil randomly reinforced with glass + macromesh + basalt fiber at Dr = 30% and Dr = 50% are shown in Figure 17, and the reinforcement depth-bearing capacity ratio relationship is given in Figure 18.

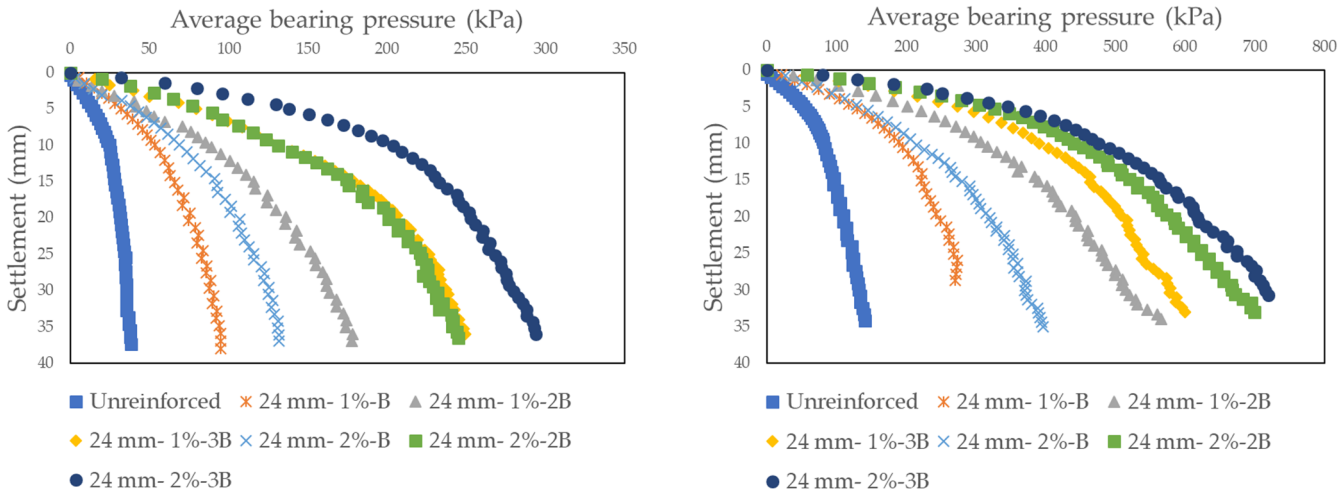


Figure 17. Average base pressure-settlement curves obtained as a result of model tests on sand soil randomly reinforced with glass + macromesh + basalt fiber: (**a**) Dr = 30%, Fl = 24 mm; (**b**) Dr = 50%, Fl = 24 mm.

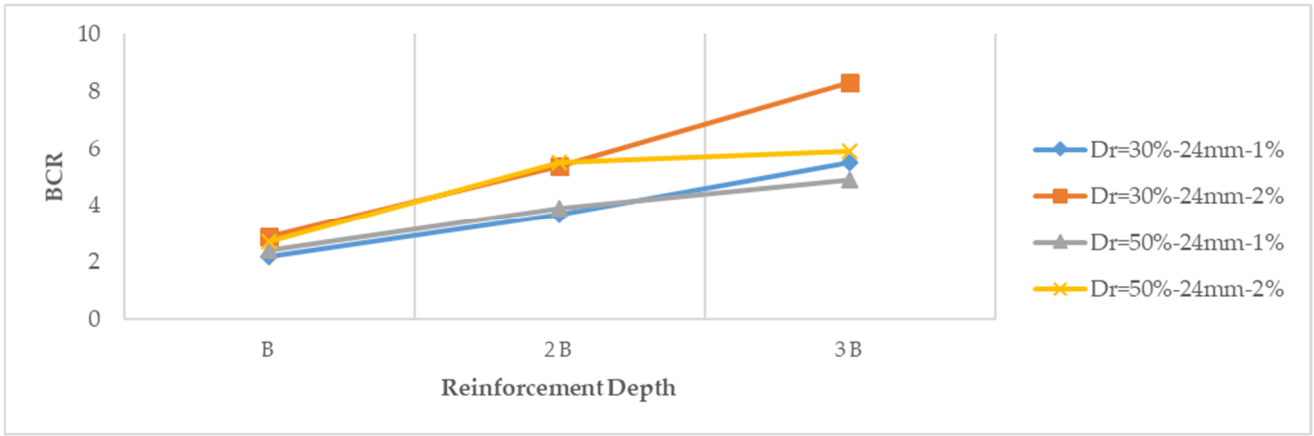


Figure 18. Variation of bearing capacity ratio (BCR) with reinforcement depth (Dr = 30–50%, Fl = 24 mm, Fc = 1–2%, glass + micromesh + basalt fiber).

- In glass + macromesh + basalt fiber-reinforced soils, the highest ultimate bearing capacity (q_u) was determined as 475 kPa in the case of adding glass + macromesh + basalt fiber to the sand at Dr = 50%, Fc = 2%, Fl = 24 mm, and 3B reinforcement depth. The highest BCR was determined as 8.3 by adding glass + macromesh + basalt fiber to sand at Dr = 30%, Fc = 2%, Fl = 24 mm, 3B reinforcement depth.
- Depending on the fiber additive ratio, a decrease in the amount of increase in the bearing capacity ratio was seen as the depth of layers grew. In tests with glass + basalt + macromesh fiber added with Dr = 50% relative density, 2B reinforcement depth can be preferred.

3.1. The Effect of Different Fiber Additives on Soil Behavior

The graphs obtained within the scope of the study as a result of evaluating together the different fiber types (glass, basalt, and macromesh fiber), hybrid fiber (glass + basalt, glass + macromesh, basalt + macromesh, and glass + basalt + macromesh fiber), fiber length (Fl = 24 mm and Fl = 48 mm), fiber content (Fc = 1% and Fc = 2%), relative density (Dr = 30% and Dr = 50%) and reinforcement depth (B, 2B and 3B) is given in Figures 19 and 20. The BCR values obtained as a result of the tests are also given in Table 5.

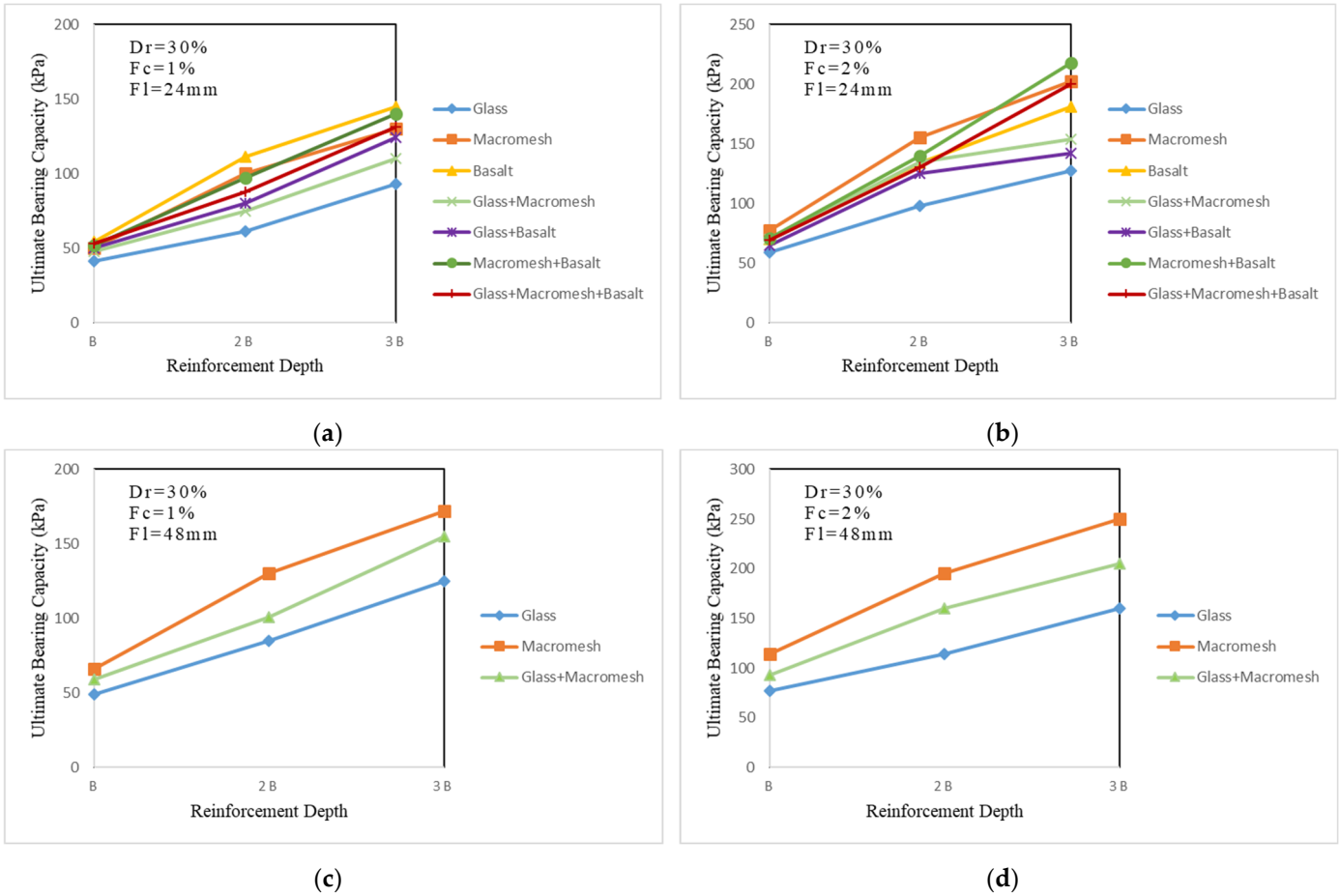


Figure 19. Reinforcement depth-ultimate bearing capacity relationship corresponding to fiber type in tests with Dr = 30% relative density: (**a**) fiber content 1%, fiber length 24 mm; (**b**) fiber content 2%, fiber length 24 mm; (**c**) fiber content 1%, fiber length 48 mm; (**d**) fiber content 2%, fiber length 48 mm.

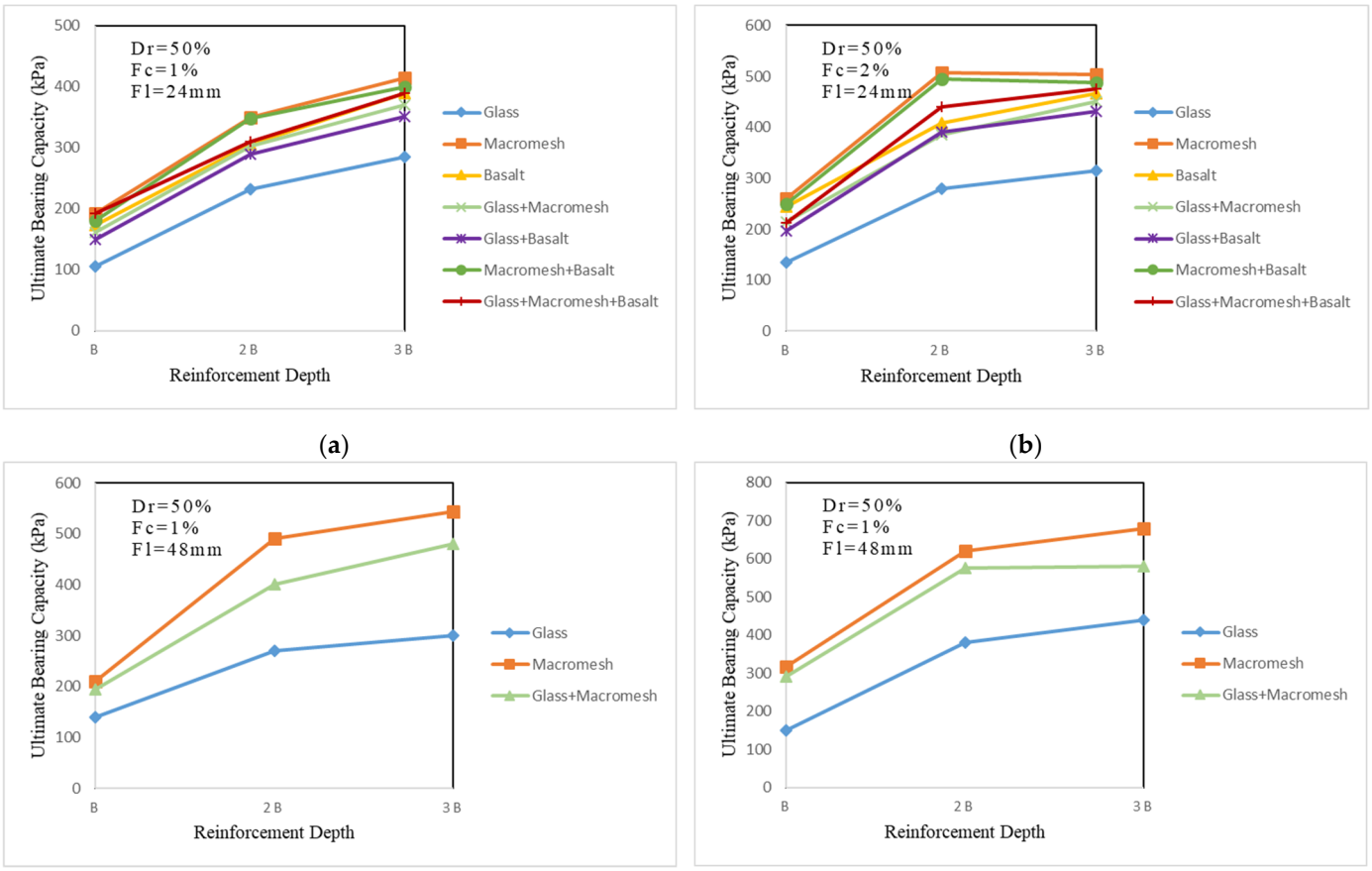


Figure 20. Reinforcement depth-ultimate bearing capacity relationship corresponding to fiber type in tests with Dr = 50% relative density: (**a**) fiber content 1%, fiber length 24 mm; (**b**) fiber content 2%, fiber length 24 mm; (**c**) fiber content 1%, fiber length 48 mm; (**d**) fiber content 2%, fiber length 48 mm.

Table 5. BCR values obtained as a result of tests.

			Glass		Macromesh		Basalt		Glass + Macromesh		Glass + Basalt		Macromesh+ Basalt		Glass + Basalt + Macromesh	
			30%	50%	30%	50%	30%	50%	30%	50%	30%	50%	30%	50%	30%	50%
24 mm	1%	B	1.7	1.3	2.1	2.4	2.2	2.2	2.0	2.0	2.1	1.9	2.2	2.3	2.2	2.4
		2B	2.5	2.9	4.2	4.4	4.6	3.8	3.1	3.8	3.3	3.6	4.0	4.4	3.7	3.9
		3B	3.9	3.6	5.4	5.2	6.0	4.9	4.6	4.6	5.2	4.4	5.8	5.0	5.5	4.9
	2%	B	2.5	1.7	3.2	3.2	2.9	3.1	2.9	2.7	2.7	2.5	3.0	3.1	2.9	2.7
		2B	4.1	3.5	6.5	6.4	5.6	5.1	5.6	4.8	5.2	4.9	5.8	6.2	5.4	5.5
		3B	5.3	3.9	8.4	6.3	7.5	5.8	6.4	5.6	5.9	5.4	9.0	6.1	8.3	5.9
48 mm	1%	B	2.0	1.8	2.8	2.6			2.5	2.4						
		2B	3.5	3.4	5.4	6.1			4.2	5.0						
		3B	5.2	3.8	7.2	6.8			6.5	6.0						
	2%	B	3.2	1.9	4.8	4.0			3.9	3.6						
		2B	4.8	4.8	8.1	7.8			6.7	7.2						
		3B	6.7	5.5	10.4	8.5			8.5	7.3						

A thorough review of the literature revealed that the use of fibers in geotechnical engineering is applicable in six fields, including pavement layers (road construction), retaining walls, railway embankments, protection of slopes, earthquake, and soil-foundation engineering. According to an existing study, the Bradshaw Field Training Area in Australia's Northern Territory stabilized aprons, taxiways, and a helipad using Portland cement and PP fibers. According to some researchers, the use of fibers in conjunction with geogrids can make it easier and more affordable to build tall vertical walls for railway embankments in low-lying residential areas. Additionally, because they can accept the irregular shape of failed slopes, soil mixtures containing randomly distributed fibers can be employed as patches in the localized repair of slope failures. The fiber reinforcement can eliminate the necessity for an anchorage that is present with planar reinforcement and also lessens gully erosion in the reinforcement of soil veneer, such as landfill covers [46].

In the case of using random fiber reinforcement to improve the soil properties, the differences in the results obtained according to the type of fiber selected as reinforcement are significant [47]. Three different fiber types were used in experimental studies. These fibers are glass fiber, basalt fiber, and macromesh fiber, respectively. Glass fiber and macromesh fiber were used in two different lengths of 24 mm and 48 mm, while basalt fiber was used only in 24 mm length. Therefore, in the comparison of these fibers, experimental groups made with a length of 24 mm were evaluated. As can be seen in Figure 19a, using basalt fibers as reinforcement with Dr = 30%, Fl = 24 mm, and Fc = 1% yielded higher ultimate bearing capacity values compared to the use of glass fiber and macromesh fiber at all reinforcement depths. In other groups, the ultimate bearing capacity values of macromesh fiber-added soils are higher than basalt and glass fiber-added soils. Strength increases are related to the shear stresses that occur in the soil as a result of the incorporation of fibers into the soil, revealing the tensile strength of the fibers. Liu et al. [48] investigated the effect of fiber additives of different types (polypropylene, basalt, and glass) on the mechanical performance of sand, similar to our study. When the results were examined, polypropylene fiber with the same content gave more strength to the treated floor due to its good flexible structure and strength properties compared to other fibers. Malidarreh et al. [49] reported that the better interconnection properties of polypropylene fiber also contribute to the ductility gain. In addition, the superiority of macromesh fiber-reinforced samples compared to glass and basalt fiber-reinforced samples is due to the higher surface roughness. Tagnit-Hamou et al. [50] and Tang et al. [51] studies, they reported that the fiber reinforcement mechanism is based on friction and the roughness of the surface of the fibers strongly affects the sand fiber interaction. A fiber's original surface roughness has an impact on how well its strength is mobilized by nearby soil particles. Hard sand particles that touch the fiber surface during the cutting process cut abrade it, causing plastic deformation and even the loss of a portion of the surface layer. The development of holes and grooves on the surface of the fiber increases the interactions between that surface and the sand matrix by forming an interlock. Compared to basalt fiber and glass fiber macromesh fiber, their positive effects on strength increase were more limited as they have a smoother surface.

When the experimental results with hybrid fibers are examined, as observed in the separate use of the fibers, the increase in the relative density, the increase in the depth of reinforcement, the increase in the fiber additive ratio from 1% to 2%, and the increase in the fiber length have positively affected the increase in the ultimate bearing capacity value. In Zhang et al. [36], Ghadakpour et al. [52] and Soltani et al. [53]'s studies, it has been stated that the simultaneous use of fibers with different lengths and aspect ratios (hybrid) improves soil properties more effectively than a single fiber. However, in the experiments, the ultimate bearing capacity values obtained from the soils with macromesh fiber additives are mostly higher than the ultimate bearing capacity values obtained from the soils with hybrid fiber additives. Among the hybrid experimental groups, the highest ultimate bearing capacity was obtained from the group reinforced at 3B depth, Dr = 30%, Fc = 2%, and in which basalt and macromesh fiber were used together. In addition, the

ultimate bearing capacities obtained from the glass fiber-reinforced tests were lower than all the other fibers used. However, much higher qu values were obtained when basalt and macromesh were mixed with fiber. When hybrid fiber-reinforced soils are evaluated, it has been observed that when glass fiber is used together with basalt or macromesh fiber, dispersibility is better than when only glass fiber is added to the soil. With sufficient content and length, two or more fibers form a good spatial network structure in the soil [30,34]. Due to the differences in fiber diameters, large-diameter fiber forms a large-scale spatial skeleton structure, while small-diameter fiber created a smaller scale spatial structure, and the combination of the two gave better results in soil reinforcement [37,54].

3.2. The Effect of Fiber Length on Soil Behavior

In this study, glass fiber and macromesh fiber were used in two different lengths of 24 mm and 48 mm, and the effect of the length of the fibers on the bearing capacity was investigated. In order to examine the effect of fiber length on ultimate bearing capacity, 36 experimental groups were evaluated. Looking at the results, it was observed that the increase in fiber length increased the ultimate bearing capacity in both glass fiber and macromesh fiber added tests and glass + macromesh fiber added tests. Chen et al. [24] and Tran et al. [55], in their previous studies, stated that the increase in fiber length positively affects the carrying capacity. Fiber length affects the reinforcing effect by affecting the contact area, but this effect is relatively small compared to the fiber content. In addition, Moghal et al. [56] reported that the increase in carrying capacity with the increase in fiber length was associated with the surface morphology of the fiber. When glass fiber and macromesh fiber are compared among themselves, it was observed that the macromesh fiber-reinforced soil bearing capacity increased more as a result of the increase in fiber length. As seen in the experimental study, since the outer surface of the macromesh fiber is rougher than the glass fiber, the resistance created on the surface of the fiber increased as the fiber length increased. As the fiber length increases, the bonding and friction force between the fiber and soil grains increases, and the bearing capacity increases. The shear strength of the soil increases due to the tensile force formed as a result of the friction force between the fiber and soil grains. Tabakouei et al. [57] said that the bridging effect of the fibers increases as the fiber length increases. According to Liang et al. [58], their study reported that when exposed to an external force, the effect between fibers of different lengths and the soil takes different forms of failure. When the fiber length is short, the failure patterns are characterized by shearing or slipping of the fiber. As the fiber length increases, the failure patterns are characterized by fiber breakage. However, excessively long fiber makes uniform fiber distribution in soil difficult. Because, in long fibers soil, this can cause agglomeration and uneven distribution. As a result, when the length of the fibers used to strengthen the soil is extended, more energy must be spent for a certain deformation to occur in the soil. When the experimental groups were examined among themselves, the effect of fiber length was seen mostly in the tests (49%) reinforced with Dr = 50%, Fc = 2%, glass + macromesh fiber at 2B depth, and it was seen in the tests (48%) reinforced with Dr = 30%, Fc = 2%, macromesh fiber at B depth, and it was seen in the tests (40%) rein-forced with Dr = 50%, Fc = 2%, glass fiber at 3B depth.

3.3. The Effect of Fiber Content on Soil Behavior

Within the scope of the study, fiber reinforcement was added to the soil at two different additive rates 1% and 2% by weight, and the effect of the fiber additive ratio on the bearing capacity was investigated. The fiber contents determined in the experimental study were selected as a result of the studies in the literature. When the fiber content is increased from 1% to 2%, it has been observed that the ultimate bearing capacity increases. When the fiber content does not exceed a certain amount, the fiber is effectively dispersed. As the fiber content increases, it affects the contact area between the fiber and the soil, affecting the cohesion and friction between the fiber and the soil. Similar observations were made by Zafar et al. [59] on natural and synthetic fiber-reinforced soil. Therefore, when the fiber

content was increased from 1% to 2%, a larger contact area occurred in the soil and improved mechanical properties. When the tests were examined among themselves, the effect of fiber content was mostly obtained from tests with glass + macromesh fiber reinforcement (80%) with Dr = 30% Fl = 24 mm, reinforcement depth 2B, and it was obtained from tests (73%) with macromesh fiber reinforcement with Dr = 30% Fl = 48 mm, reinforcement depth B. However, as the fiber ratio increased, difficulties began to be experienced in placement. In addition, as the fiber content increased, it was observed that the amount of increase in the bearing capacity ratio decreased, especially in model tests performed at Dr = 50% relative density. If the fiber content is increased too much, the fibers may begin to show a tendency to agglomerate. As a result, the fibers do not effectively increase the contact area. They can reduce the effectiveness of the fiber by creating a weak surface in the soil. These results are consistent with those found by Tabakouei et al. [57]. According to Prabakar and Sridhar [60], increasing the fiber content above a certain point lessens the interaction between soil particles and, as a result, results in less cohesion being mobilized, which lowers the shear strength of the fiber soil composite. Therefore, the contribution rate was not increased above 2% in the tests. In addition, when the fibers were evaluated among themselves, the increase in the bearing capacity with the increase in fiber content was observed in the macromesh fibers the most. This is mostly related to the dispersibility of the fiber [61]. Even after the glass fibers are added to the soil and mixed well, they are mostly dispersed in the soil in bundles. This reduces the benefit to be gained from increased fiber content. Although basalt fibers showed better dispersibility than glass fiber, they were not as effective as macromesh fiber.

3.4. The Effect of Reinforcement Depth on Soil Behavior

Within the scope of the experimental study, the soils were equipped with 1, 2, and 3 times the width of the foundation under the foundation plate. To examine the effect of the reinforced soil layer depth on the bearing capacity, the determined experimental groups were evaluated. Determining the optimum reinforcement depth in soils is an important parameter to design and build a more economical structure. As the depth of the reinforced soil from the foundation base increased, the ultimate bearing capacity of the soil increased has also been reported before by other researchers such as Li et al. [62], Doğan Küçükçongar et al. [63]. In the model loading tests performed at Dr = 30%, the ultimate bearing capacity increased proportionally as the reinforcement depth increased. At Dr = 50%, changing the depth of reinforcement from B to 2B resulted in significant increases in bearing capacity, but when changed from 2B to 3B, the rate of increase in bearing capacity decreased. When compared according to fiber types, as the reinforcement depth increases, the increase in ultimate bearing capacity was highest in glass fiber-reinforced tests and least in macromesh-reinforced tests. In model tests with Dr = 50% Fl = 24 mm Fc = 2% macromesh fiber reinforced and Dr = 50% Fl = 24 mm Fc = 2% basalt + macromesh fiber-reinforced tests, there was no increase in ultimate bearing capacity when the reinforcement depth was increased from 2B to 3B. Therefore, at Dr = 50%, it is considered sufficient to reinforce the 2B depth from the foundation base. It has been observed that the soil under strip footing and the ideal reinforcement depth are between 2B and 3B according to the varying relative density values [63,64].

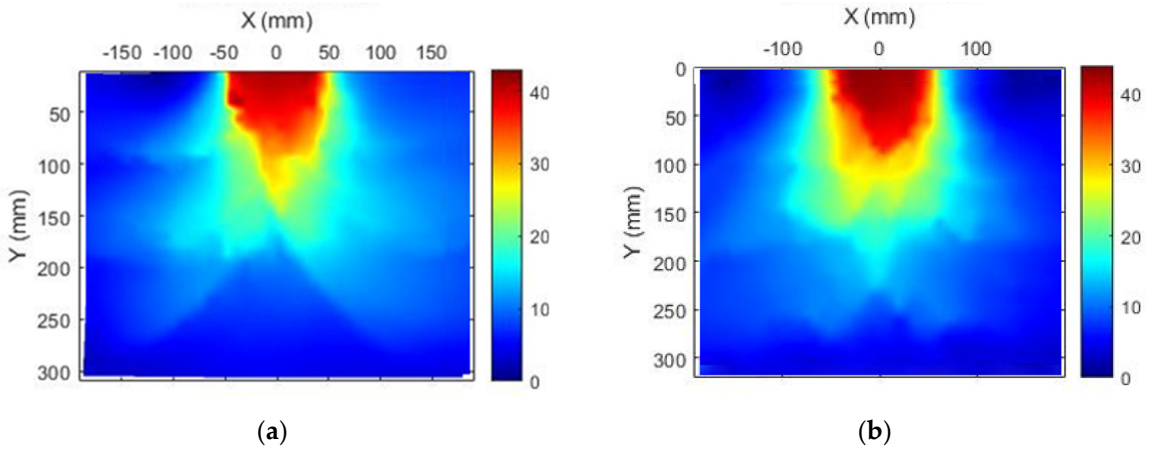
3.5. The Effect of Relative Density on Soil Behavior

In the study, unreinforced and reinforced tests were carried out in loose and medium-dense sand with Dr = 30% and Dr = 50%. Tests to examine the effect of relative density on bearing capacity were evaluated. In all tests, increases in ultimate bearing capacity occurred when Dr = 30% increased to 50%. Different relative densities mean different dry densities. In previous studies on fiber-reinforced sand with different dry densities, it was stated that the stiffness and bearing capacity of the fiber-reinforced soil with higher dry density were higher [65]. In addition, the interfacial movement between the fiber and the soil increases significantly with increasing relative stiffness [54]. A larger relative density

means smaller porosity and smaller porosity means increased cohesion and friction as a result of increased contact area between fiber and soil particles. Similar observations were made by Belkhatir et al. [66] on fiber-reinforced soil. The authors reported that a high relative density causes a further increase in the effective contact area between soil particles and fiber. Yixian et al. [67] and Li-Hua et al. [68] indicated that increasing the relative density and increased fiber deformation increased the mechanical interaction between fiber and soil. Thus, it can be noted that the relative density positively affects the soil's mechanical behavior. In the reinforced tests, the bearing capacity ratios obtained in the tests performed at Dr = 30% relative density at all fiber types, fiber length, fiber percentage, and reinforcement depths were higher than the bearing capacity ratios obtained from the tests performed at Dr = 50% relative density. Maximum bearing capacity ratios according to relative density were: BCR = 6.7 at Dr = 30%, BCR = 5.5 at Dr = 50% for glass fiber; BCR = 7.5 at Dr = 30%, BCR = 5.8 at Dr = 50% for basalt fiber; BCR = 10.4 at Dr = 30%, and BCR = 8.5 at Dr = 50% for macromesh fiber. It is seen that the effect of reinforcement is more effective in loose soils [69]. The highest increase in ultimate bearing capacity was determined as 280% in glass fiber-reinforced tests with Fl = 24 mm Fc = 1% reinforcement depth 2B; as 277% in the tests with macromesh fiber reinforcement with Fl = 48 mm Fc = 1% reinforcement depth 2B, and as 286% from the tests with macromesh fiber reinforcement with Fl = 24 mm Fc = 1% reinforcement depth B. Especially in soils reinforced with 2B and 3B depths, as the relative density increased, the ultimate bearing capacities increased significantly.

3.6. GeoPIV Analysis Results

The analysis of pictures taken while the tests were carried out to monitor the deformation at the time of collapse and the formation of the slip band in the unreinforced and reinforced model tests in the soil under different conditions were analyzed using the PIV method. To use this method, GeoPIV-RG, an image analysis module designed for geotechnical research applications running under the MATLAB R2019B program was used [70]. First, the image analysis of the tests carried out on unreinforced soil was made. Afterward, PIV analyses of the experimental groups with 1% and 2% fiber content at 30% relative density were performed, and the PIV analyses of the experimental groups with 1% and 2% fiber content at 50% relative density were performed, respectively. Although the images obtained according to the fiber type are similar, the analysis results obtained from the macromesh fiber-added soils, which have the greatest effect on the bearing capacity in general, are given. The shear strain images resulting from the PIV analyses are shown in Figures 21 and 22.



(**a**) (**b**)

Figure 21. *Cont.*

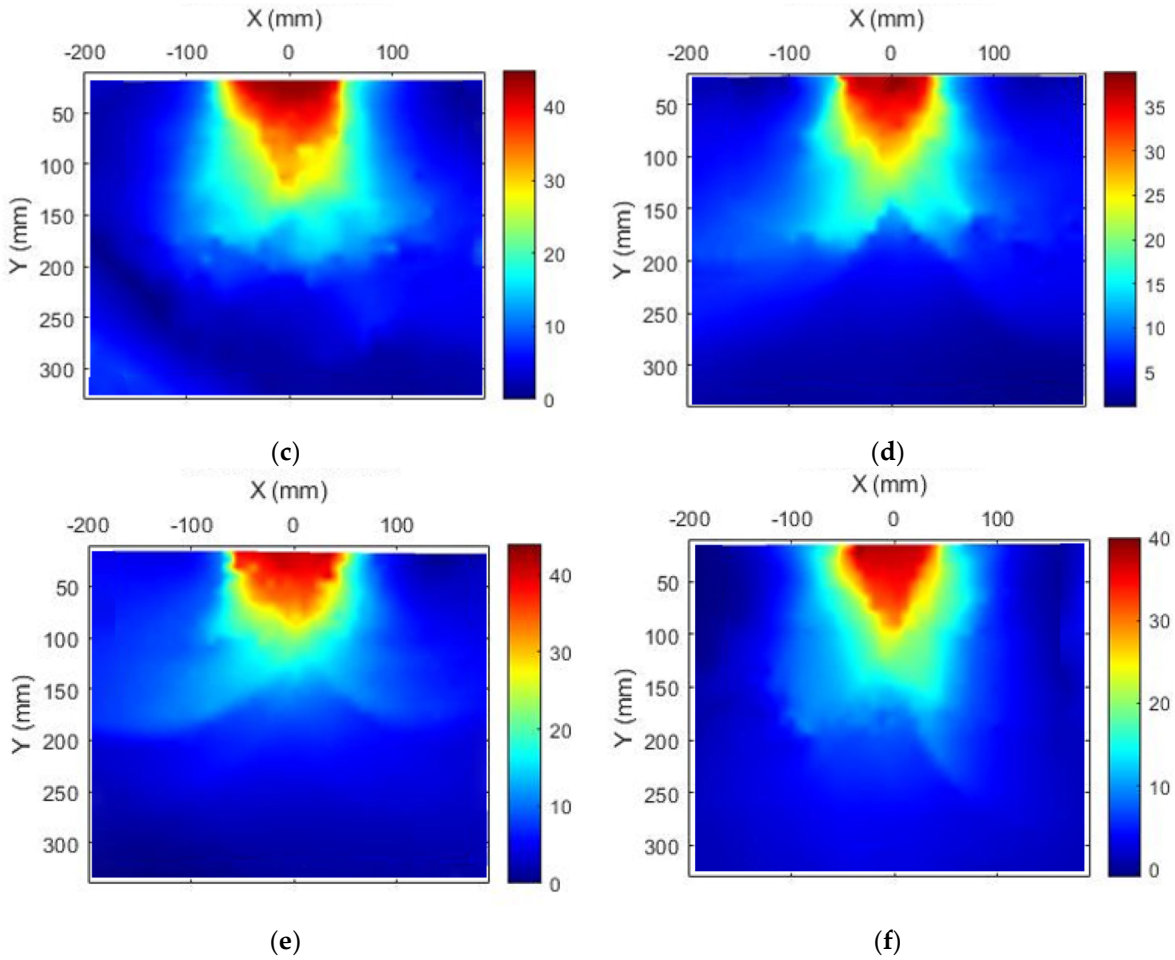


Figure 21. PIV results with Dr = 30%: (**a**,**b**) Unreinforced; (**c**,**d**); Fiber content 1%; (**e**,**f**) Fiber content 2%.

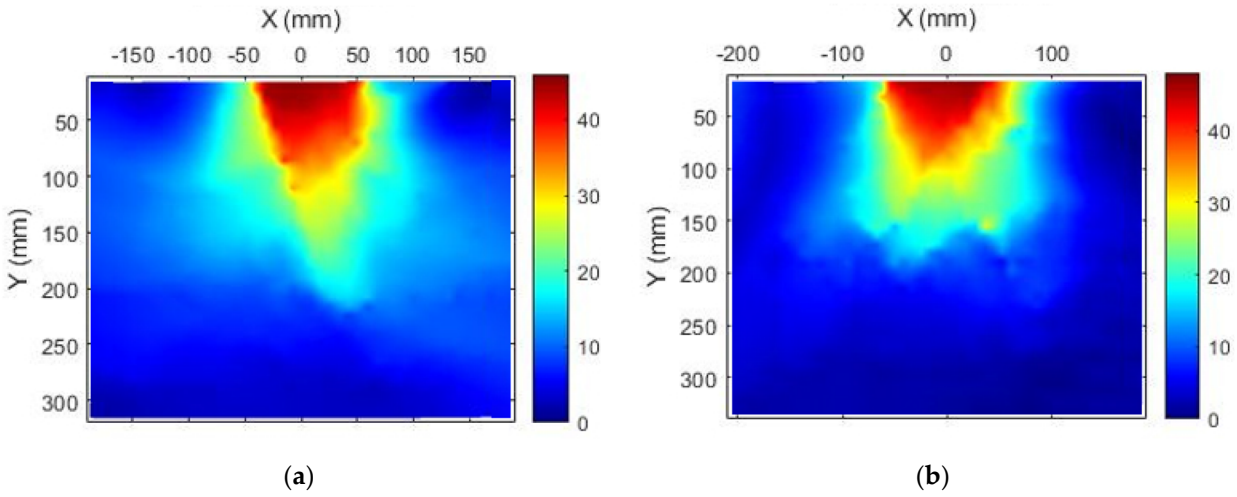


Figure 22. *Cont.*

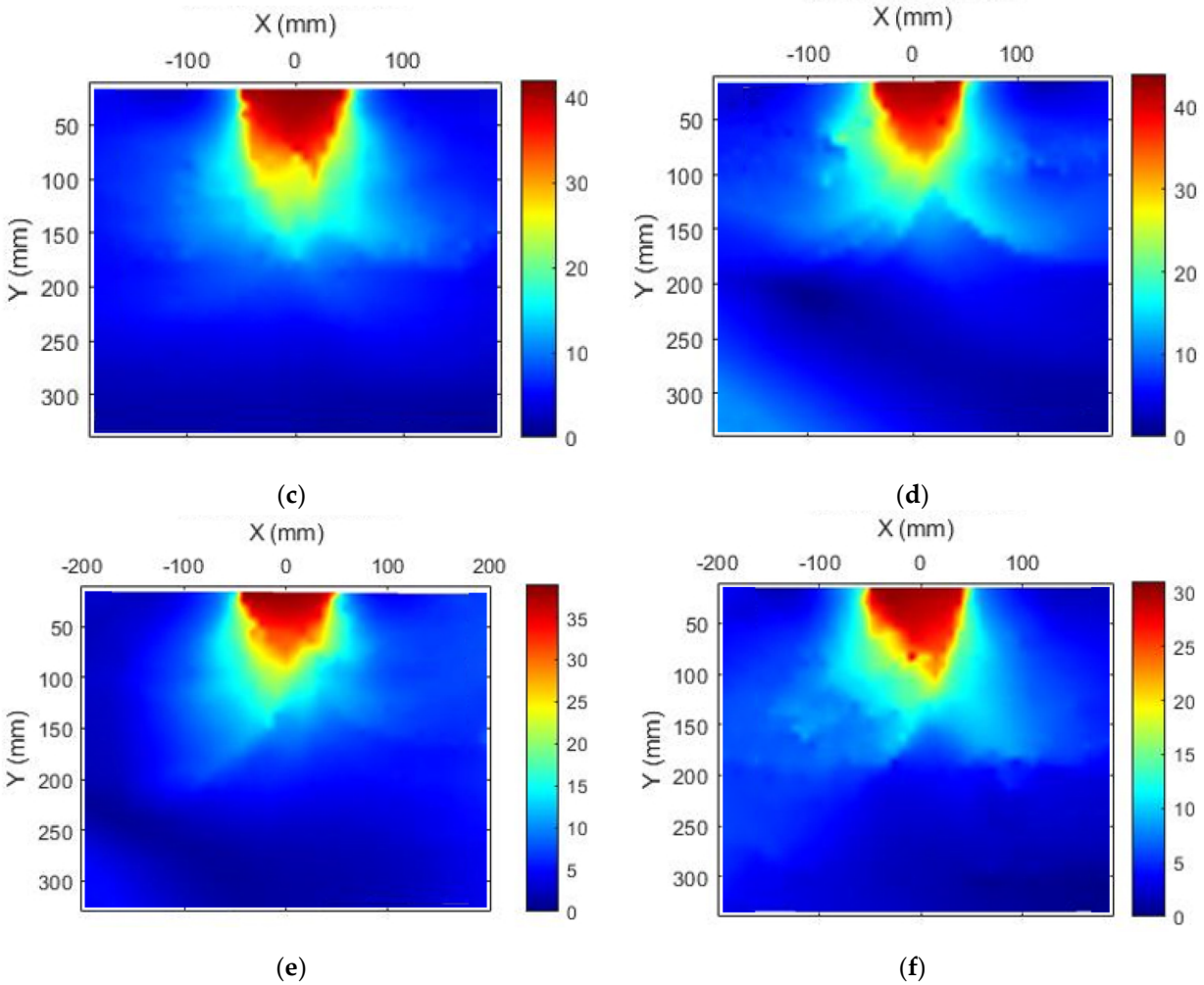


Figure 22. PIV results with Dr = 50%: (**a**,**b**) Unreinforced; (**c**,**d**); fiber content 1%; (**e**,**f**) fiber content 2%.

When the analyses were examined, it was seen that the grain movement in the unreinforced soil was deeper than in the reinforced soil. When the data on reinforced soils were evaluated, it was observed that the displacement decreased as the relative density increased. In general, it can be said that with the increase in the relative density and increasing the fiber reinforcement ratio from 1% to 2%, the displacement decreases and the effect of the loads from the foundation is not transmitted to deeper [45]. In unreinforced model tests, shear surfaces at Dr = 30% relative density were observed to form as punching shear failure, and slip surfaces at Dr = 50% relative density were observed to form as a local shear failure. When reinforcement is added to the unreinforced soil, the slip surfaces of the soil go from a punching shear failure to a local shear failure at Dr = 30% soil. When the percentage of reinforcement was increased from 1% to 2%, the stresses were distributed over a larger area, and a larger area was affected on the right and left sides of the foundation. In general, the addition of reinforcement to the soil transferred the stresses in the soil to a larger area that was observed in the current paper in the case of fiber-reinforced specimens has also been reported before by other researchers such as Çelik et al. [71], Yazdandoust et al. [72]. In this way, the area over which the stress is distributed has increased and it has been observed that the ultimate bearing capacity is higher in reinforced soils than in unreinforced soils.

Limitations and Future Work

Since basalt fiber with a length of 48 mm could not be supplied in the study, the effect of fiber length could not be investigated in the basalt fiber-added experimental groups. In hybrid fiber groups, the fibers were limited by mixing them at the same length and in equal proportions. In the future, the fibers used in the studies to be carried out with random

hybrid fibers can be added to the soil at different percentages, and model tests can be made. The effects of hybrid fibers, which will be prepared by using fibers of different lengths, on soil behavior can be investigated by laboratory and field tests. In addition to the fibers used in the study, the use of different fibers as hybrid reinforcement in the ground can be investigated.

4. Conclusions

1. It has been observed that the effect of macromesh fiber on improving the strength properties of the soil is higher than basalt and glass fiber.
2. It was observed that the increase in fiber length and fiber percentage increased the ultimate bearing capacity.
3. When the situation where glass fiber and basalt fiber are added separately to the soil and the use of macromesh fiber in the hybrid form are compared, it is seen that the hybrid fiber has positive effects on soil bearing capacity.
4. BCR values obtained as a result of reinforcement with fiber are higher in soils with low relative density. It is seen that the positive effect of reinforcement with fiber reinforcement is greater in loose soils.
5. It has been observed that the soil under strip footing and the ideal reinforcement depth are between 2B and 3B according to the varying relative density values.
6. As a result of the PIV analyses, when the fiber is added to the unreinforced soil, it was seen that the settlement in the soil decreases and the effect of the loads coming from the foundation is not transmitted to deeper.

Author Contributions: Conceptualization, B.A.A. and S.Ç.; methodology, B.A.A. and S.Ç.; software, B.A.A.; validation, B.A.A. and S.Ç.; formal analysis, B.A.A. and S.Ç.; investigation, B.A.A. and S.Ç.; resources, B.A.A.; data curation, B.A.A.; writing—original draft preparation, B.A.A.; writing—review and editing, B.A.A.; visualization, B.A.A.; supervision, S.Ç.; project administration, B.A.A. and S.Ç.; funding acquisition, B.A.A. All authors have read and agreed to the published version of the manuscript.

Funding: This research received no external funding.

Institutional Review Board Statement: Not applicable.

Informed Consent Statement: Not applicable.

Data Availability Statement: The data presented in this study are available upon request from the corresponding author.

Conflicts of Interest: The authors declare no conflict of interest.

References

1. Vidal, H. The principle of reinforced earth. *Highw. Res. Rec.* **1966**, *282*, 1–16.
2. Waldron, L. The shear resistance of root-permeated homogeneous and stratified soil. *Soil Sci. Soc. Am. J.* **1977**, *41*, 843–849. [CrossRef]
3. Jamshidi, R.; Towhata, I.; Ghiassian, H.; Tabarsa, A. Experimental evaluation of dynamic deformation characteristics of sheet pile retaining walls with fiber reinforced backfill. *Soil Dyn. Earthq. Eng.* **2010**, *30*, 438–446. [CrossRef]
4. Ghiassian, H.; Jamshidi, R.; Tabarsa, A. Dynamic performance of Toyoura sand reinforced with randomly distributed carpet waste strips. In *Geotechnical Earthquake Engineering and Soil Dynamics IV*; ASCE: Reston, WV, USA, 2008; pp. 1–13.
5. Gray, D.H.; Ohashi, H. Mechanics of fiber reinforcement in sand. *J. Geotech. Eng.* **1983**, *109*, 335–353. [CrossRef]
6. Yetimoglu, T.; Salbas, O. A study on shear strength of sands reinforced with randomly distributed discrete fibers. *Geotext. Geomembr.* **2003**, *21*, 103–110. [CrossRef]
7. Hataf, N.; Rahimi, M. Experimental investigation of bearing capacity of sand reinforced with randomly distributed tire shreds. *Constr. Build. Mater.* **2006**, *20*, 910–916. [CrossRef]
8. Yetimoglu, T.; Inanir, M.; Inanir, O.E. A study on bearing capacity of randomly distributed fiber-reinforced sand fills overlying soft clay. *Geotext. Geomembr.* **2005**, *23*, 174–183. [CrossRef]
9. Mukherjee, K.; Mishra, A.K. Impact of glass fibre on hydromechanical behaviour of compacted sand–bentonite mixture for landfill application. *Eur. J. Environ. Civ. Eng.* **2021**, *25*, 1179–1200. [CrossRef]

10. Patel, S.K.; Singh, B. Shear strength response of glass fibre-reinforced sand with varying compacted relative density. *Int. J. Geotech. Eng.* **2019**, *13*, 339–351. [CrossRef]
11. Patel, S.K.; Singh, B. A comparative study on shear strength and deformation behaviour of clayey and sandy soils reinforced with glass fibre. *Geotech. Geol. Eng.* **2020**, *38*, 4831–4845. [CrossRef]
12. Sujatha, E.; Atchaya, P.; Darshan, S.; Subhashini, S. Mechanical properties of glass fibre reinforced soil and its application as subgrade reinforcement. *Road Mater. Pavement Des.* **2021**, *22*, 2384–2395. [CrossRef]
13. Philley, P.D.; Kalita, A.; Omo, Y. Improvement of Strength Behaviour of Fly Ash and Cement Stabilized Soil with Glass Fibre Reinforcement. In *Advances in Geo-Science and Geo-Structures*; Springer: Singapore, 2022; pp. 133–142.
14. Benziane, M.M.; Della, N.; Sert, S.; Denine, S.; Nouri, S.; Bol, E.; Elroul, A.B. Shear behaviour of sandy soil from Chlef river reinforced with different types of fibres. *Mar. Georesources Geotechnol.* **2022**, *40*, 1232–1241. [CrossRef]
15. Lv, X.; Zhou, H.; Liu, X.; Song, Y. Experimental study on the effect of basalt fiber on the shear behavior of cemented sand. *Environ. Earth Sci.* **2019**, *78*, 688. [CrossRef]
16. Kale, R.; Neha, D.; Sakshi, M.; Gaurav, A.; Pranit, J.; Vaishnavi, R.; Chetan, R. Soil stabilization by using basalt fibers. *Int. J. Sci. Res. Eng. Trends* **2020**, *6*, 1931–1935.
17. Gobinath, R.; Mahesh, V.; Shyamala, G.; Rajesh, A. Strength and Settlement studies on basalt fiber reinforced marginal soil. In *IOP Conference Series, Proceedings of the International Conference on Recent Advancements in Engineering and Management (ICRAEM-2020), Warangal, India, 9–10 October 2020*; IOP Publishing: Philadelphia, PA, USA, 2020; p. 032083.
18. Gao, C.; Du, G.; Guo, Q.; Zhuang, Z. Static and dynamic behaviors of basalt fiber reinforced cement-soil after freeze-thaw cycle. *KSCE J. Civ. Eng.* **2020**, *24*, 3573–3583. [CrossRef]
19. Wang, S.; Chen, F.; Xue, Q.; Zhang, P. Splitting tensile strength of cement soil reinforced with basalt fibers. *Materials* **2020**, *13*, 3110. [CrossRef]
20. Boz, A.; Sezer, A.; Özdemir, T.; Hızal, G.E.; Azdeniz Dolmacı, Ö. Mechanical properties of lime-treated clay reinforced with different types of randomly distributed fibers. *Arab. J. Geosci.* **2018**, *11*, 122. [CrossRef]
21. Ndepete, C.P.; Sert, S.; Beycioğlu, A.; Katanalp, B.Y.; Eren, E.; Bağrıaçık, B.; Topolinski, S. Exploring the effect of basalt fibers on maximum deviator stress and failure deformation of silty soils using ANN, SVM and FL supported by experimental data. *Adv. Eng. Softw.* **2022**, *172*, 103211. [CrossRef]
22. Xu, J.; Wu, Z.; Chen, H.; Shao, L.; Zhou, X.; Wang, S. Triaxial shear behavior of basalt fiber-reinforced loess based on digital image technology. *KSCE J. Civ. Eng.* **2021**, *25*, 3714–3726. [CrossRef]
23. Mukhtar, M.; Kumar, E.A. To Study the Behavior of Compacted Soil Using Basalt Fibers. *Int. J. Innov. Res. Eng. Manag.* **2022**, *9*, 360–366.
24. Chen, W.; Zhao, J.; Fan, L.; Li, J.; Yuan, B.; Li, H.; Jiang, G.; Li, H.; Chen, T. The effect of length and content of fiber on glass fiber and basalt fiber-reinforced granite residual soil. *Adv. Civ. Eng.* **2022**, *2022*, 7803002. [CrossRef]
25. Latifi, M.R.; Biricik, Ö.; Mardani Aghabaglou, A. Effect of the addition of polypropylene fiber on concrete properties. *J. Adhes. Sci. Technol.* **2022**, *36*, 345–369. [CrossRef]
26. Wang, Q.; Ding, Y.; Zhang, Y.; Castro, C. Effect of macro polypropylene fiber and basalt fiber on impact resistance of basalt fiber-reinforced polymer-reinforced concrete. *Struct. Concr.* **2021**, *22*, 503–515. [CrossRef]
27. Rostami, R.; Zarrebini, M.; Abdellahi, S.B.; Mostofinejad, D.; Abtahi, S.M. Investigation of flexural performance of concrete reinforced with indented and fibrillated macro polypropylene fibers based on numerical and experimental comparison. *Struct. Concr.* **2021**, *22*, 250–263. [CrossRef]
28. Brasse, K.; Tracz, T.; Zdeb, T. The Effect of the Type and Amount of Synthetic Fibers on the Effectiveness of Dispersed Reinforcement in Soil-Cements. *Materials* **2020**, *13*, 3917. [CrossRef] [PubMed]
29. Daneshfar, M.; Hassani, A.; Aliha, M.; Berto, F. Investigating Flexural Performance of Fiber-Reinforced Concrete with Different Contents and Types of Macrosynthetic Fiber. *Strength Mater.* **2022**, *54*, 650–661. [CrossRef]
30. Badri, M.Z.A.; Khalid, F.S. Performance of concrete containing combination of macro mesh PP and nylon fibers. *Recent Trends Civ. Eng. Built Environ.* **2021**, *2*, 475–481.
31. Akın, S.K.; Kartal, S.; Müsevitoğlu, A.; Sancıoğlu, S.; Zia, A.J.; Ilgün, A. Macro and micro polypropylene fiber effect on reinforced concrete beams with insufficient lap splice length. *Case Stud. Constr. Mater.* **2022**, *16*, e01005. [CrossRef]
32. Khan, M.; Cao, M.; Xie, C.; Ali, M. Hybrid fiber concrete with different basalt fiber length and content. *Struct. Concr.* **2022**, *23*, 346–364. [CrossRef]
33. Khan, M.; Cao, M.; Xie, C.; Ali, M. Efficiency of basalt fiber length and content on mechanical and microstructural properties of hybrid fiber concrete. *Fatigue Fract. Eng. Mater. Struct.* **2021**, *44*, 2135–2152. [CrossRef]
34. Ding, Y.; Wang, Q.; Pacheco-Torgal, F.; Zhang, Y. Hybrid effect of basalt fiber textile and macro polypropylene fiber on flexural load-bearing capacity and toughness of two-way concrete slabs. *Constr. Build. Mater.* **2020**, *261*, 119881. [CrossRef]
35. Zhang, J.; Xu, W.; Gao, P.; Su, L.; Kun, B.; Yueyuan, L.; Bohan, Y. Integrity and crack resistance of hybrid polypropylene fiber reinforced cemented soil. *J. Eng. Fibers Fabr.* **2022**, *17*, 15589250211068428. [CrossRef]
36. Zhang, J.; Xu, W.; Gao, P.; Yao, Z.; Su, L.; Qiu, N.; Huang, W. Compressive strength characteristics of hybrid fiber-reinforced cemented soil. *Int. J. Pavement Eng.* **2022**, 1–27. [CrossRef]
37. Shu, Y.; Zhang, J. Effect of Basalt Fiber Content and Length on the Strength and Crack Development of Polyvinyl Alcohol/Basalt Hybrid Fiber-Reinforced Cement Soil. *Polymers* **2023**, *15*, 2146. [CrossRef]

38. *ASTM D2487-17*; Standard Practice for Classification of Soils for Engineering Purposes (Unified Soil Classification System). ASTM International: West Conshohocken, PA, USA, 2020.
39. *ASTM D3080-04*; Standard Test Method for Direct Shear Test of Soils Under Consolidated Drained Conditions. ASTM International: West Conshohocken, PA, USA, 2012.
40. Briaud, J.-L.; Jeanjean, P. Load settlement curve method for spread footings of sand. In *Vertical and Horizontal Deformations of Foundations and Embankments*; ASCE: Reston, WV, USA, 1994; pp. 1774–1804.
41. Trautmann, C.H.; Kulhawy, F.H. Uplift load-displacement behavior of spread foundations. *J. Geotech. Eng.* **1988**, *114*, 168–184. [CrossRef]
42. De Beer, E. Experimental determination of the shape factors and the bearing capacity factors of sand. *Geotechnique* **1970**, *20*, 387–411. [CrossRef]
43. Ateş, B.; Şadoğlu, E. Kum zeminlerdeki kazıklı radye temellerin optimum kazık aralığının deneysel olarak incelenmesi. *Tek. Dergi* **2021**, *32*, 10477–10494. [CrossRef]
44. Stanier, S.A.; Blaber, J.; Take, W.A.; White, D. Improved image-based deformation measurement for geotechnical applications. *Can. Geotech. J.* **2016**, *53*, 727–739. [CrossRef]
45. Xu, L.; Chen, H.-b.; Chen, F.-q.; Lin, Y.-j.; Lin, C. An experimental study of the active failure mechanism of narrow backfills installed behind rigid retaining walls conducted using Geo-PIV. *Acta Geotech.* **2022**, *17*, 4051–4068. [CrossRef]
46. Hejazi, S.M.; Sheikhzadeh, M.; Abtahi, S.M.; Zadhoush, A. A simple review of soil reinforcement by using natural and synthetic fibers. *Constr. Build. Mater.* **2012**, *30*, 100–116. [CrossRef]
47. Kravchenko, E.; Liu, J.; Niu, W.; Zhang, S. Performance of clay soil reinforced with fibers subjected to freeze-thaw cycles. *Cold Reg. Sci. Technol.* **2018**, *153*, 18–24. [CrossRef]
48. Liu, J.; Bai, Y.; Song, Z.; Kanungo, D.P.; Wang, Y.; Bu, F.; Chen, Z.; Shi, X. Stabilization of sand using different types of short fibers and organic polymer. *Constr. Build. Mater.* **2020**, *253*, 119164. [CrossRef]
49. Malidarreh, N.; Shooshpasha, I.; Mirhosseini, S.; Dehestani, M. Effects of reinforcement on mechanical behaviour of cement treated sand using direct shear and triaxial tests. *Int. J. Geotech. Eng.* **2018**, *12*, 491–499. [CrossRef]
50. Tagnit-Hamou, A.; Vanhove, Y.; Petrov, N. Microstructural analysis of the bond mechanism between polyolefin fibers and cement pastes. *Cem. Concr. Res.* **2005**, *35*, 364–370. [CrossRef]
51. Tang, C.; Shi, B.; Gao, W.; Chen, F.; Cai, Y. Strength and mechanical behavior of short polypropylene fiber reinforced and cement stabilized clayey soil. *Geotext. Geomembr.* **2007**, *25*, 194–202. [CrossRef]
52. Ghadakpour, M.; Choobbasti, A.J.; Kutanaei, S.S. Investigation of the Kenaf fiber hybrid length on the properties of the cement-treated sandy soil. *Transp. Geotech.* **2020**, *22*, 100301. [CrossRef]
53. Soltani, A.; Deng, A.; Taheri, A. Swell–compression characteristics of a fiber–reinforced expansive soil. *Geotext. Geomembr.* **2018**, *46*, 183–189. [CrossRef]
54. Li, J.; Tang, C.; Wang, D.; Shi, B.; Pei, X. Single fiber pullout tests on interfacial shear strength of wave-shape fiber-reinforced soils. *Chin. J. Geotech. Eng.* **2014**, *36*, 1696–1704.
55. Tran, K.Q.; Satomi, T.; Takahashi, H. Effect of waste cornsilk fiber reinforcement on mechanical properties of soft soils. *Transp. Geotech.* **2018**, *16*, 76–84. [CrossRef]
56. Moghal, A.A.B.; Chittoori, B.C.; Basha, B.M.; Al-Shamrani, M.A. Target reliability approach to study the effect of fiber reinforcement on UCS behavior of lime treated semiarid soil. *J. Mater. Civ. Eng.* **2017**, *29*, 04017014. [CrossRef]
57. Tabakouei, A.R.; Narani, S.; Abbaspour, M.; Aflaki, E.; Siddiqua, S. Coupled specimen and fiber dimensions influence measurement on the properties of fiber-reinforced soil. *Measurement* **2022**, *188*, 110556. [CrossRef]
58. Liang, S.; Xiao, X.; Wang, J.; Wang, Y.; Feng, D.; Zhu, C. Influence of fiber type and length on mechanical properties of MICP-treated sand. *Materials* **2022**, *15*, 4017. [CrossRef] [PubMed]
59. Zafar, T.; Ansari, M.A.; Husain, A. Soil stabilization by reinforcing natural and synthetic fibers–A state of the art review. *Mater. Today Proc.* **2023**, *in press*. [CrossRef]
60. Prabakar, J.; Sridhar, R. Effect of random inclusion of sisal fibre on strength behaviour of soil. *Constr. Build. Mater.* **2002**, *16*, 123–131. [CrossRef]
61. Duong, N.T.; Tran, K.Q. Estimation of seepage velocity and piping resistance of fiber-reinforced soil by using artificial neural network-based approach. *Neural Comput. Appl.* **2023**, *35*, 2443–2455. [CrossRef]
62. Li, J.; Zhou, C.; Xin, G.; Long, G.; Zhang, W.; Li, C.; Zhuang, P.; Yao, Z. Study on reinforcement mechanism and reinforcement effect of saturated soil with a weak layer by DC. *Appl. Sci.* **2022**, *12*, 9770. [CrossRef]
63. Doğan Küçükçongar, Ş.; Çelik, S.; Karimi Ghalehjough, B. Experimental and Numerical Investigation for Estimating Optimal Depth-Bearing Capacity of Randomly Fiber-Reinforced Sandy Soils. *J. Sci. Ind. Res.* **2022**, *81*, 1037–1049.
64. Li, L.; Xiao, H.; Gao, M.; Liu, Y.; Hu, Z.; Yao, K. Experimental investigations on effect of geocell, waste tire chips, and geocell–tire chips on foundation reinforcement. *J. Perform. Constr. Facil.* **2019**, *33*, 04019074. [CrossRef]
65. Brahimi, A.; Bouri, D.E.; Boutaraa, Z.; Nougar, B.; Krim, A.; Chemmam, M.; Arab, A. Numerical and experimental study on the effect of fiber reinforcement on the shear strength and hydraulic conductivity of Chlef soil. *Innov. Infrastruct. Solut.* **2023**, *8*, 40. [CrossRef]
66. Belkhatir, M.; Schanz, T.; Arab, A.; Della, N.; Kadri, A. *Insight into the Effects of Gradation on the Pore Pressure Generation of Sand-Silt Mixtures*; ASTM International: Oxford, UK, 2014.

67. Yixian, W.; Panpan, G.; Shengbiao, S.; Haiping, Y.; Binxiang, Y. Study on strength influence mechanism of fiber-reinforced expansive soil using jute. *Geotech. Geol. Eng.* **2016**, *34*, 1079–1088. [CrossRef]
68. Li, L.; Liu, S.; Xiao, H.; Feng, W.; Li, J.; Wu, P. Experimental investigation on reinforcement effect of sustainable materials for different subgrades. *J. Clean. Prod.* **2022**, *343*, 130944. [CrossRef]
69. Fazeli Dehkordi, P.; Ghazavi, M.; Karim, U.F. Bearing capacity-relative density behavior of circular footings resting on geocell-reinforced sand. *Eur. J. Environ. Civ. Eng.* **2022**, *26*, 5088–5112. [CrossRef]
70. Stanier, S.; Dijkstra, J.; Leśniewska, D.; Hambleton, J.; White, D.; Wood, D.M. Vermiculate artefacts in image analysis of granular materials. *Comput. Geotech.* **2016**, *72*, 100–113. [CrossRef]
71. Çelik, S.; Ghalehjough, B.K.; Majedi, P.; Akbulut, S. Effect of randomly fiber reinforcement on shear failure surface of soil, behind flexible retaining walls at different conditions. *Indian J. Geo-Mar. Sci.* **2017**, *46*, 2097–2104.
72. Yazdandoust, M.; Taimouri, A.B.B. Lateral Pressure Distribution and Shear Band Development in Two-Tiered MSE Walls under Footing Loading. *Int. J. Geomech.* **2023**, *23*, 04023038. [CrossRef]

Disclaimer/Publisher's Note: The statements, opinions and data contained in all publications are solely those of the individual author(s) and contributor(s) and not of MDPI and/or the editor(s). MDPI and/or the editor(s) disclaim responsibility for any injury to people or property resulting from any ideas, methods, instructions or products referred to in the content.